

Pending recovery in the strength of the meridional overturning circulation at 26°N

Ben. I. Moat¹, David. A. Smeed¹, Eleanor Frajka-Williams¹, Damien G. Desbruyères², Claudie Beaulieu³, William E. Johns⁴, Darren Rayner¹, Alejandra Sanchez-Franks¹, Molly O. Baringer⁵, Denis Volkov^{5,6}, Laura C. Jackson⁷, Harry L. Bryden⁸

We thank the reviewers for their time in commenting on this paper. We have prepared a detailed response to reviewers #1 and #2.

Reviewer 1 notes that we are relying on the expectations that (a) AMOC transport will increase as a result of strong buoyancy forcing in the subpolar North Atlantic and (b) that there is some relationship between the AMOC in the subpolar and subtropical gyres. These are indeed assumptions that we are working with as they are the prevailing view of the AMOC circulation variability on long timescales. On shorter timescales, the transport variability is confounded by higher frequency/shorter period fluctuations that are wind driven. This short timescale variability presents significant challenges in identifying meridional connectivity, particularly when time series are themselves short.

We are further relying on the assumption that meridional coherence of the circulation, if it exists, will appear in transport fluctuations (e.g., Zhang 2010, Bingham and Hughes, 2009) rather than in watermass advection (e.g., Zou et al. 2016). The arrival of watermass signatures, while easier to identify in longer hydrographic records, is a complicated integral of the transport variability along spreading paths, and represents a complementary measure of ocean circulation change.

We have attempted to identify transport covariance between the best available AMOC observations at 26N, and the longest available estimates at 45N. To extend the timeseries at 26N, we have used the GloSea5 reanalysis which was shown to capture the interannual variability of the RAPID array at 26N albeit with reduced amplitude (Jackson et al. 2019). Using these records, we still cannot conclude a definitive lead-lag relationship between two latitudes. However, we anticipate that the strong subpolar cooling in 2013-2015 may provide an impulse response that will generate a signal in meridional connectivity above the background high frequency ‘noise’.

The GloSea5 time series has been extended to the end of 2018 by Laura Jackson at the UK Met Office, and is now included in this paper (red line Figure 6a). Laura has also contributed to the analysis in the updated paper so we have included her as a co-author.

Anonymous referee #1

Detailed responses to particular points follow:

1) If a strengthening of the subpolar water mass transformation leads an increasing AMOC at 45N by 5-6 years (line 193 in this manuscript). Then why did the AMOC at 45N already begin to increase around 2011 (Figure 6a)?

Desbruyeres et al. (2019) and the AMOC time series at 45N show an increase from a relative minimum in 2010. Similarly, the watermass transformation shows an increase from a relative minimum in 2005 (5 years earlier). However, the watermass transformation due to oceanic heat loss was not significantly greater than zero until 2010. We have updated the text in the manuscript to read:

“These localised deep convection events are part of wider and longer-term intensification in subpolar water mass transformation that was at a minimum in 2005”

2) Recent Lagrangian studies, however, show much longer time scales (> 10 years) for those dense waters to be exported to the subtropics (e.g., Jackson et al. 2016; Zou et al. 2016). A more comprehensive discussion will be needed to reconcile those different perspectives on how the subpolar water mass transformation may impact overturning variability.

Lagrangian approaches identify advective pathways between the subpolar and subtropical regions in the Atlantic, but are not ideal to capture faster boundary wave-mediated changes in transport. Indeed, Zou et al (2016) comments on this issue after finding that the Lagrangian approach did not show any relationship between watermass formation and transport variability. To get around this, they used e-floats on either side of key latitudes to match the transport anomaly signatures, finding that it propagated much more quickly than water parcels did (2 year time lag).

We have added text to emphasize that with our transport time series we are looking at how anomalies in transport propagate meridionally, rather than how water parcels propagate meridionally.

“Lagrangian studies have been used to identify when newly formed dense waters from the subpolar gyre reach the subtropics, with anomalies moving with the currents via advection (e.g., Bower et al., 2009; Zou et al., 2016; Jackson et al., 2015). However, transport time series can also adjust more rapidly through a fast boundary-wave mediated response of lower latitude AMOC variability to high latitudes forcing. Such a response can potentially be identified by lag correlation or coherence analysis of AMOC transport time series, rather than hydrographic anomalies. Based on the increase in subpolar watermass transformation peaking in 2013-2015 and various time lags between the subpolar-to-subtropical AMOC strength determined from numerical simulations, we would anticipate a sign of the increasing subtropical AMOC by 2018-2022.”

3) The authors then suggested that a larger AMOC at 45N leads a larger AMOC at 26N by 0-2 years. But using the same GloSea5, Jackson et al. (2016) suggested that the AMOC anomalies at 45N precedes 26N by about 10 years. How to reconcile such a significant discrepancy? Is it related to the use of the observed AMOC at 45N and the modeled AMOC at 26N?

We agree that this is an inconsistency that cannot yet be reconciled from the observations. Given the short duration of the records available and the conflicting time lags identified within GloSea (26N to 45N) itself and between GloSea5 26N and observational estimates at 45N, we are removing the ‘0-2 year’ lag estimate and replacing it with, ‘consistent with a possible 0-2 year lag’.

“With the relatively short duration records and the absence of a clear impulse anomaly to track between latitudes, it is not yet possible to identify the timescale of adjustment between the subpolar and subtropical AMOC strength. It appears, however, from comparing the 45°N observational estimate of the AMOC and 26°N from GloSea5, that the adjustment timescale may be short (0-2 years). In contrast, within the GloSea5 reanalysis itself there was a mean lag of 7 years between a peak in Labrador Sea density and the AMOC at 26°N (Jackson et al., 2015). This discrepancy is difficult to reconcile. While GloSea5 has been validated against the 26°N observations, there does not exist an equivalent long AMOC record in the subpolar gyre to verify GloSea5: the OSNAP estimate of the AMOC is too short (21 months) to verify interannual variability of reanalyses (Lozier et al., 2019) and the method used at 45°N with altimetry and gridded hydrography may be subject to errors particular in resolving higher frequency anomalies at the boundary. “

4) In addition, the authors cited Zou et al. (2019) on the connection between the subpolar UNADW and subtropical LNADW transport anomalies. Note that Zou et al. (2019) suggested that such a latitudinal AMOC connection can be due to gyre-dependent forcing; only strong LNADW transport anomalies can propagate southward from the subpolar region to the subtropics in 4 years. A discussion on this and a reconciliation with the presented analysis are currently missing in the manuscript.

The analysis in Zou et al (2019) relies on a single large anomaly during a relative short model run (1991-2004). They find that for this single large anomaly, that a UNADW transport anomaly in the subpolar gyre leads to a subtropical LNADW anomaly 4 years later. This timescale is, however, inconclusive even within their paper where they have 3 different analysis with three different timescales. We don't believe there is anything substantially new to reconcile with our analysis, as we do not separate 45N into layers, and our AMOC anomalies at 26N are (as they are in Zou et al. 2019, and previous RAPID papers) due to anomalies in LNADW. We have therefore removed this reference to Zou et al. 2019.

5) AMOC-AMV-subpolar OHC relationships. It is a bit confusing about the relationships of AMOC-AMV-subpolar OHC. The authors first suggested that the AMOC lead the AMV by ~5 years as shown in a high-resolution model (Moat et al. 2019), but then pointed out the AMOC maximum at 45N precedes the AMV by ~10 years in GloSea5 (lines 243-244 in this manuscript). Does it imply that the AMOC-AMV relationship is just model-specific?

Moat et al., (2019) shows that in a high resolution model the AMOC leads the AMV by ~5 years at 26N and ~9 years at 50N (Moat et al. 2019, figure 3a), which broadly agrees with the reviewers comment above. Although Moat et al., (2019) found these correlations to be significant at the 95% level, they do not account for all the AMV variability ($R^2 = 0.33$) and other processes could contribute to the variability independent of the AMOC, e.g. Atmospheric teleconnections from the tropics, and variability of the Arctic sea ice and snow cover. From this study the AMOC leading does seem to be robust. Given the short length of the time series in observations we cannot yet be sure about the absolute lag between the AMOC at 45N and 26N. Here we are presenting the broad scale response of the North Atlantic to changes in the AMOC at 26N.

In addition, how does the AMOC-AMV relationship relate to the subpolar OHC changes?

A paper on the full heat budget of the North Atlantic is currently being written by the authors, so we have removed the discussion on the ocean heat content changes from this manuscript.

6) The authors suggested a relationship between the weakened heat transport in the sub-tropics (i.e., in relation to a weak AMOC state) and the cooling subpolar gyre during 2013-2015. Should it be focused on the heat transport at 45N that is at the southern boundary of the subpolar gyre?

45N is spanning the subpolar gyre and intergyre-gyre region, so there is no clear break between the subtropical and subpolar gyres. While 26N is near the middle rather than the north of the subtropical gyre (Fig 1), it is expected that AMOC fluctuations in the subtropical gyre are coherent, so that the heat transport through the middle of the subtropical gyre is proportional to the heat transport through the northern edge of the subtropical gyre (Zhang 2010, Bingham & Hughes 2009).

Another manuscript is in preparation to do a detailed heat budget for the North Atlantic. We are therefore reducing references to the heat transport variability, including removing the OHC time series in Fig 6b.

7) The AMOC at 45N appears to be strengthening after 2011 (Figure 6a), indicating an increasing northward heat transport during the cooling period. How to exclude the impact from the strengthened atmospheric forcing during 2013-2015 (e.g., de Jong and de Steur 2016)? My suggestion is to add a timeseries of the surface heat flux over the subpolar region during the overlapping period of 1985-2018 and discuss accordingly their potential impact on the oceanic changes. Otherwise, in my opinion, it is hard to draw any conclusions on how the AMOC changes lead the changes in the subpolar OHC.

Desbruyeres et al. (2019) discuss the heat budget in the North Atlantic. They use the time-accumulated MHT relative to a reference period from 1996-2013 and determine that the OHC anomaly is initially entirely explained by MHT, and then (during the development of the cold blob) is not. The time-accumulated quantity is, however, sensitive to the choice of reference period; using a different reference period (1993-2017) results in a change in slope of the time-accumulated quantity (integral of a constant with time is a trend).

As we are presently involved in another, more detailed, heat budget analysis, we don't believe we can add significantly to what Debruyeres et al. (2019) already showed.

Other Comments:

8) Lines 162-163: To utilize the lengthy record, the authors could put error bars on the monthly values and comment on how robust the seasonal cycles are.

This has been done. we have updated figure 3 and added the following to the text:

“There is a substantial seasonal cycle with an amplitude of 2.0 ± 0.16 Sv and 0.7 ± 0.16 Sv (mean and standard deviation from Monte Carlo estimation) for the annual and semi-annual harmonic, explaining 11% and 2% of the variance, respectively. The residual timeseries, likewise, retains substantial variability with a range of 21.6 Sv and a standard deviation of 3.4 Sv. About 20% of the residual variance is associated with the estimated error of ± 1.5 Sv for the 10-day binned data.”

9) Lines 180-181: Need more information on Figure 5. How to understand the different change points defined by Mean+CP and Trend+CP? Mean+CP shows an earlier change point around 2008. Also, it is not clear from Figure 5 why Mean+AR(1)+CP is the overall best fit. Please add more details on how this was determined.

More details explaining the methodology and how the best model is selected have been added in Section 3.2:

“For the models with changepoints, we find the number and locations using the pruned exact linear time algorithm (Killick et al., 2012), which performs an exact search considering all options for any possible number of changepoints and select the optimal number/location balancing the overall fit against the length of each segment. The most appropriate model is selected according to the Akaike Information Criteria (AIC). The AIC differences between each model included in the comparison and the model with the smallest AIC are also computed to assess plausibility of all models. As a rule of thumb, a difference larger than 10 indicates that there is essentially no support for a model given the data and the other models at play (Beaulieu & Killick, 2018). To verify sensitivity to the choice of information criterion, the Bayesian Information Criterion for each model is also computed.”

Given that the AIC differences between each model and the one with the smallest AIC are all large (>10), we can conclude that no other model amongst those compared fit the data reasonably well.

10) Line 184: The standard deviation clearly varies with the time scales over which it is derived. I would suggest the authors show the standard error in the mean instead, which seems to be more helpful when determining how distinct the time-mean transports are between two years or any two periods.

We have quoted the standard error in the text. The values in Table 1 have been left as the standard deviation as this is more relevant to the AMOC variability, but we have added the de-correlation time scales into the Table 1 caption to enable the standard error to be calculated if required.

11) Line 189: Is section 4.2 just about the relationship to 45N? If so, better to be more specific.

Title of section 4.2 has been changed to ‘AMOC relationship between 26°N and 45°N’

12) Lines 190-203: Please see my main concern point 1).

This has been addressed above in point 1).

13) Line 208: Is the timing of the AMOC increase at 45N (2010-2011) sensitive to the size of the filter?

The timing should not be sensitive to the filtering. Desbruyeres et al. (2019) made a quick test on how their comparison AMOC was influenced by the filtering and concluded that: Lowpass filtered time series presented throughout the paper use a 7-year Hanning window and endpoints are therefore truncated at ± 3 years. The impact of low-pass filtering AMOC and SFOC time series on the lagged auto-correlations were studied by varying the size of the filtering window (0, 3, 5, 7, 9 and 11 years). While the raw annual time series show small correlations at all lags ($R < 0.4$), maximum correlations for smoothing windows of 3 years and above were reached at a consistent lag of 5-6 years.

14) Lines 213-214: Is the difference in the variability the same between the AMOC at 45N and 26N both in GloSea5?

Like the observations the AMOC- Ekman using GloSea5 at 45N (in density space) does have higher variability than GloSea5 at 26N, but GloSea5 at 45N does have slightly less variability than observation at 45N. The standard deviation of the AMOC- Ekman in GloSea5 at 45N is 1.02 Sv and at 26N is 0.63 Sv. The standard deviation of the observations is 1.58 Sv (45N) and 0.77 Sv (26N).

As we do not make reference to the GloSea5 time series at 45N we have removed the line, "With these two time series, the variability in the GloSea5 estimate of AMOC-Ekman at 26°N is more markedly lower than at 45°N."

15) Line 238: The authors appear to emphasize a 5-year time lead by the AMOC. But I couldn't find any observational evidence even in this analysis for such a time lead.

The 5 year time lead is from a coupled climate study by Moat et al. (2019), calculated using fields over a 300 year period. Given the short length of the high quality time series at RAPID 26N (2004 to 2018) is it hard to directly show this lag between AMOC and AMV. In this paper (figure 6) using the GloSea5 reanalysis we show that AMOC leading AMV is robust, but there is a bit of variation in the precise lags.

We have rewritten Section 4.3 to make the description of the lead lag relationship between the AMOC, AMV and NAO clearer.

16) Lines 253-255: Please see my main concern #2.

This has been addressed above in point 2) and 15) and in the text.

Anonymous referee #2

17) However, I have some issues with the central scientific focus of the paper and felt that the general thrust of the argument was often misguided

We thank the reviewer for their detailed comments, and also their support of the RAPID 26N observations. We agree that they are the best available observations of the continuously varying AMOC, and have edited the text to improve this emphasis. However, one of this reviewer's

major disagreements with the manuscript was that we tried to put the RAPID observations in the wider North Atlantic context and that this should not have been the focus of the manuscript.

We disagree. The value of RAPID lies not only in giving the best possible estimate of AMOC transport variability at an individual latitude (of great value as a benchmark for numerical models, ocean reanalyses and ocean dynamics investigations), we believe that as the RAPID time series lengthens it is enabling us to begin to address key climate questions—the *raison d’être* for AMOC studies. These include detailed analyses of local causes of variability and regional impacts of variability, but also how the subtropical AMOC responds to buoyancy (rather than wind) forcing, what influence the AMOC has on decadal and longer variations in the Atlantic, and what the relationship is between the AMOC at different latitudes. It is clear that we are only beginning to have a long enough record to address these questions—and not yet to satisfactorily answer them.

Text has been added in two places:

- Section 2.1, first line: “The 14 years of observations at 26°N represent the most complete and longest records of the directly observed AMOC variability currently available.”
- Section 2.1, second paragraph: “The use of boundary moorings which sample at high frequency (hourly) enables high frequency (e.g. tidal and mesoscale) variability to be resolved and not aliased (Kanzow et al., 2009)”

18) I think the GloSea5 data is overused and overly trusted to give a realistic representation of the ocean. The authors attempt to reconcile the results with the 45N time series from Debruyeres et al. (2019), but I think too much respect is paid towards these results which are not of comparable stature

We have added text to clarify that the RAPID observations are the most complete and longest record of AMOC variability, but also that the 45N estimates are the longest available subpolar-area AMOC estimates. While they may be flawed, the covariability between buoyancy forcing and AMOC transport estimates in Desbruyeres et al. (2019) provides some confidence, as does the consistency between the overall findings of Desbruyeres et al. (2019) and the OSNAP programme (Lozier et al., 2019) including that watermass transformation east of Greenland is the major driver of subpolar AMOC transport variability. To provide confidence in GloSea5, Jackson et al., (2019) compared the AMOC at 26N and 50N in a large set of reanalyses and finds agreement in the variability.

Minor Comments

19) Line 27: “Comparing the two latitudes, the AMOC at 26°N is higher than its previous low” this sentence needs to better distinguish spatial and temporal changes.

We have replaced: “We have therefore examined the record of transports at 26°N to see whether the AMOC in the subtropical North Atlantic is now recovering from a previously reported low period commencing in 2009. Comparing the two latitudes, the AMOC at 26°N is higher than its previous low.”

with

“Examining 26N, we find that the AMOC is higher than its previous low, though not yet exceeding its long-term mean.”

20) Line 35: Slightly clumsy sentence, repetition of “on”

This has been changed to;

“It drives a large net northward transport of heat, with one petawatt ($1 \text{ PW} = 10^{15} \text{ W}$) released to the atmosphere between 26°N and 70°N , impacting the climate in the North Atlantic region (e.g. Srokosz et al., 2012) on surface temperatures, precipitation and sea level (Delworth and Mann, 2000).”

21) Line 71: “Guided by”. This language ties directly into point 2. RAPID should lead, not follow.

We have updated this to:

“Based on the RAPID observations and the recent findings at 45°N , we make preliminary investigations into the meridional coherence of the AMOC transport variability between 26°N and 45°N , and the response at 26°N to the impulse forcing in 2013/15.”

22) Line 83: missing “to”

This has been corrected.

23) Line 89: The heat and freshwater fluxes are mentioned here but neither shown nor discussed. Perhaps a sentence explaining why?

We have added:

“Here we focus on the volume transport; updated analyses of the heat and freshwater transports are the subject of a separate study.”

24) Line 95: Are the CTD-Os a subset of the CTDs?

No, they are in addition as the CTD-Os and only sample every 4 hours. We have clarified this in the text.

25) Line 107: “net the”

‘Net’ has been deleted.

26) Line 109: GloSea5 should be mentioned here.

The following has been added in Section 2.3

“We also use data from the GloSea5 global ocean and sea ice reanalysis (Blockley et al 2014, Jackson et al 2016), which uses the NEMO GO5 ocean model with a nominal resolution of 0.25° and with 75 vertical layers (Megann et al 2014). It assimilates in-situ and satellite sea surface temperatures; sub-surface ocean profiles of temperature and salinity; sea ice concentration; and sea level anomalies using the NEMOVAR v13 assimilation scheme (Waters et al, 2015). The experiment is described in more detail in Jackson et al. (2016), with a more in-depth comparison to observations and other ocean reanalyses in Jackson et al (2019).”

27) Line 132: missing “use”

This has been corrected.

28) Line 150: Should say “Results”

Thank you! This has been corrected.

29) Line 158: why is “anti-correlated” repeated inside the brackets?

This has been deleted.

30) Line 158: Clarify: there is no correlation information in the spectral plot.

This has been clarified :

We replaced:

“resulting in a reduction of power at the semi-annual frequency in the AMOC strength relative to the UMO. At periods longer than a year, the AMOC variability is dominated by the UMO transport”

with

“This anti-correlation is the cause of the reduced power at the semi-annual frequency in the total AMOC relative to the UMO.”

Note that an inference about anti-correlation can be made by comparing spectrum of total AMOC with the spectra of the components. If the total AMOC is less than one of the components then there must be some anticorrelation

31) Line 169: Use the LNADW acronym

This has been changed

32) Line 172: “that a reductions”

This has been fixed

33) Line 186: This sentence could be improved, just state the maximum and minimum values/times for comparison.

This has been rewritten for clarity.

“The AMOC transport in the 2017/18 year (17.8 ± 0.39 Sv) is larger than the recent minimum in 2009/10 (13.5 ± 0.36 Sv), but this does not represent a return to the high AMOC transport values near the beginning of the observational record (2005/06, 20.9 ± 0.32 Sv).”

34) Line 210: All this tells us is that GloSea5 is dynamically consistent with itself. It could still be wrong. I assume GloSea5 changes are forced by Lab sea deep convection, which we know many models get wrong, even if it does assimilate observations.

This is actually based on observations at 45N and GloSea at 26N. We are using the agreement between GloSea at 26N and RAPID at 26N to provide a view (potentially not correct) of what the longer term variability of the AMOC at 26N may have been, and comparing this against the

45N observations assuming—based on their robust agreement with the surface forced overturning in the subpolar gyre—that they are a reasonable estimate of the AMOC at this latitude. As RAPID 26N is the only array providing the length and quality of AMOC observations, we will necessarily need to look to other products to investigate meridional connectivity—at least until the OSNAP observations provide a longer term, high-quality estimate of subpolar overturning.

35) Line 232: You can, but I think this analysis seems uncoupled from the RAPID results.

The reviewer is referring to: “we can look more closely at the period of the observations and the longer records of ocean heat content and SSTs to evaluate whether the observed variations in the Atlantic, as indexed by the AMV, follow the patterns predicted by the numerical simulations.”

This is an area of significant interest and debate in AMOC/Atlantic community—is the AMOC responsible for fluctuations in the AMV? While the observed transport records are short relative to multi-decadal variability, some of the underlying processes (how the heat transport relates to OHC change) are within scope and may lead to mechanistic understanding of whether and how the AMOC influences the AMV.

36) Line 256: Be quantitative. What is the minimum fraction of the mean?

We apologise but we do not understand what the reviewer is referring to.

37) Line 266: This is the first mention of the 34.5S array (in the conclusions).

We have removed the reference to 34.5S

38) Line 272: Insert “within are analysis framework”.

We have chosen not to add this phrase in order to be more concise.

39) Line 288: Perhaps substitute “understanding” for “knowledge”.

This has been changed.

40) Figure 1: Red text on green very hard to read for colour blind people

This has been updated to bold black text.

Pending recovery in the strength of the meridional overturning circulation at 26°N

Ben. I. Moat¹, David. A. Smeed¹, Eleanor Frajka-Williams¹, Damien G. Desbruyères², Claudie Beaulieu³, William E. Johns⁴, Darren Rayner¹, Alejandra Sanchez-Franks¹, Molly O. Baringer⁵, Denis Volkov^{5,6}, [Laura C. Jackson⁷](#), Harry L. [Bryden⁸](#)

¹ National Oceanography Centre, University of Southampton Waterfront Campus, European Way, Southampton, SO14 3ZH, UK.

² Ifremer, University of Brest, CNRS, IRD, Laboratoire d'Océanographie Physique et Spatiale, IUEM, Ifremer centre de Bretagne, Plouzané, 29280, France.

³ Ocean Sciences Department, University of California Santa Cruz, CA, USA.

⁴ Rosenstiel School of Marine and Atmospheric Science, University of Miami, Miami, FL, USA.

⁵ Atlantic Oceanographic and Meteorological Laboratory, NOAA, Miami, FL, USA.

⁶ [Cooperative Institute for Marine and Atmospheric Studies, University of Miami, Miami, FL, USA.](#)

⁷ [Met Office, UK.](#)

⁸ School of Ocean and Earth Science, University of Southampton Waterfront Campus, European Way, Southampton, SO14 3ZH, UK.

Correspondence to: Ben Moat (ben.moat@noc.ac.uk)

Abstract. The strength of the Atlantic meridional overturning circulation (AMOC) at 26°N has now been continuously measured by the RAPID array over the period Apr 2004 - Sept 2018. This record provides unique insight into the variability of the large-scale ocean circulation, previously only measured by sporadic snapshots of basin-wide transports from hydrographic sections. The continuous measurements have unveiled striking variability on timescales of days to a decade, driven largely by wind-forcing, contrasting with previous expectations about a slowly-varying, buoyancy forced large-scale ocean circulation. However, these measurements were primarily observed during a warm state of the Atlantic Multidecadal Variability (AMV) which has been steadily declining since a peak in 2008-2010. In 2013-2015, a period of strong buoyancy-forcing by the atmosphere drove intense watermass transformation in the subpolar North Atlantic and provides a unique opportunity to investigate the response of the large-scale ocean circulation to buoyancy forcing. Modelling studies suggest that the AMOC in the subtropics responds to such events with an increase in overturning transport, after a lag of 3-9 years. At 45°N, observations suggest that the AMOC may already be increasing. [Examining 26°N, we find that the AMOC is no longer weakening, though the recent transport is not above the long-term mean.](#) Extending the record backwards in time at 26°N with ocean reanalysis from GloSea5, the transport fluctuations [at 26°N are consistent with a 0-2 year lag from those at 45°N](#), albeit with lower magnitude. Given the short span of time and anticipated delays in the signal from the subpolar to subtropical gyres, it is not yet possible to determine whether the subtropical AMOC strength is recovering [nor how the AMOC at 26°N responds to intense buoyancy forcing.](#)

- Style Definition: Normal
- Style Definition: Heading 1
- Style Definition: Heading 2
- Style Definition: Heading 3
- Style Definition: Heading 4
- Style Definition: Betreff
- Style Definition: Bullets
- Style Definition: Header
- Style Definition: Kontakt
- Style Definition: Name
- Style Definition: Copernicus_Word_template
- Style Definition: MS title
- Style Definition: List Paragraph
- Style Definition: Affiliation
- Style Definition: Equation
- Style Definition: Footer
- Style Definition: Correspondence
- Formatted: Space Before: 0 pt, Line spacing: single
- Formatted: Superscript
- Deleted: Bryden⁶
- Formatted: Not Superscript/ Subscript
- Formatted: Space Before: 0 pt
- Formatted: Space Before: 0 pt, After: 0 pt
- Deleted: ,
- Deleted: 6

- Deleted: We have therefore examined the record of transports at
- Deleted: to see whether
- Deleted: in the subtropical North Atlantic
- Deleted: now recovering from a previously reported low period commencing in 2009. Comparing the two latitudes, the AMOC at 26°N
- Deleted: higher than its previous low.
- Deleted: follow
- Deleted: by 0-2 years
- Deleted: 1¶
- Formatted: Font color: Black
- Formatted: Normal, Border: Top: (No border), Bottom: (No border), Left: (No border), Right: (No border), Between : (No border), Tab stops: 7.96 cm, Centered + 15.92 cm, Right

1 Introduction

The Atlantic Meridional Overturning Circulation (AMOC) is a large-scale circulation pattern spanning the Atlantic from south to north, transporting warm waters northward and colder waters southward. It drives a large net northward transport of heat, with one petawatt (1 PW = 10^{15} W) released to the atmosphere between 26°N and 70°N, impacting the climate in the North Atlantic region (e.g. Srokosz et al., 2012) including surface temperatures, precipitation and sea level (Delworth and Mann, 2000). The deeper limb of the AMOC is isolated from the atmosphere and can store energy and matter for centuries. Changes to the AMOC during the paleoclimate period are thought to explain the abrupt shifts in climate found in paleoclimate records (e.g., Barber et al., 1999; Ganopolski and Rahmstorf, 2001), and the current generation of coupled climate models predicts a slowing of the AMOC over the present century in response to increasing greenhouse gases (IPCC, 2013).

This widespread interest in the Atlantic circulation led to the installation of the RAPID-MOCHA-WBTS array (hereafter referred to as the RAPID 26°N array) which has now been in operation, making continuous measurements of the large-scale circulation for more than 15 years (Frajka-Williams et al., 2019). Given its role in climate, the AMOC was previously thought to be slowly varying, on 'climate' timescales (decadal and longer), and so the ocean and climate communities were surprised when the first published data from RAPID 26°N demonstrated large-amplitude variability on sub-annual timescales (Cunningham et al., 2007). Subsequent releases of the data, following the recovery and redeployment of instruments, yielded new insights into seasonal (Kanzow et al., 2010), interannual (McCarthy et al., 2012) variability, and an observed long-term decline of the AMOC at 26°N through 2016 (Smeed et al., 2014; Smeed et al., 2018). One remarkable finding from the RAPID array was the apparent dominance of wind-forcing on the annual cycle as well as the sustained dip in the AMOC strength in 2009-2010 (Roberts et al., 2013; Zhao and Johns, 2014a; Zhao and Johns, 2014b), calling into question the community's prior expectation that the large-scale overturning circulation is primarily driven by buoyancy forcing at high latitudes (Lozier 2010).

The observations to-date have mostly occurred during a warm period of the multidecadal changes in the large-scale North Atlantic, as indicated by the Atlantic Multidecadal Variability (AMV, Zhang et al., 2019). While definitions for this index vary, they generally agree that the AMV was positive (warm) during a period spanning the late 1990s, peaking around 2008-2010, then declining towards zero and even negative values (cool) depending on the definition of the AMV used (Frajka-Williams et al., 2017; Zhang et al. 2019). Numerical investigations into the relationship between the AMOC and AMV demonstrate a causal link with the AMOC driving changes in the AMV, where the northward heat transport by the AMOC accumulates in North Atlantic and generates a positive ocean temperature (subsurface and surface) anomaly that is indexed by the AMV (Moat et al., 2019). The decline from a peak in 2008-2010 occurred just prior to a cold anomaly in the subpolar North Atlantic, termed the 'cold blob', and driven partly by intense subpolar heat loss in the winters of 2013/14 and 2014/15 (Duchez et al., 2016; Josey et al., 2018) and also by reduced northward heat transport by the AMOC over a longer period leading up to the cold blob (Bryden et al., 2020). This cold anomaly heralds both a cooler state in the multidecadal variability, but also provides a large-amplitude 'impulse'-like forcing to the large-scale ocean, in a region with known sensitivity of the AMOC (Robson et al., 2014).

Formatted: Space After: 5 pt

Deleted: with far-reaching impacts on

Deleted: on

Deleted: .

Deleted: ,

Deleted: next

Deleted: lower frequency fluctuations

Deleted:) in the basin-wide transports at 26°N.

Deleted: a decline

Deleted: in large part

Deleted: air-sea buoyancy fluxes

Deleted: 2

Formatted: Font color: Black

Formatted: Normal, Border: Top: (No border), Bottom: (No border), Left: (No border), Right: (No border), Between : (No border), Tab stops: 7.96 cm, Centered + 15.92 cm, Right

90 While the subpolar AMOC has been observed since 2014 by the OSNAP array (Lozier et al., 2019), the record is as yet too
short to compare the overturning and surface forcing both during and prior to the period of intense forcing (2013-15). However,
a multi-dataset estimate of the AMOC at 45N indicates broad agreement between the surface forcing and overturning strength,
with the overturning responding to the surface forcing with a lag of 5 years and on timescales of 5 years and longer
(Desbruyeres et al., 2019). This record of the overturning strength indicates a strong increase in the AMOC at 45N, with the
increase notably commencing before the period of strongest surface heat loss.

95 Here we report on the latest AMOC transport time series at 26°N from April 2004 through the end of August 2018. We give
an overview of the variability of the AMOC transport using the complete record, including the seasonal cycle and interannual
variability, as well as the contributions of component parts of the circulation (Florida Current/Gulf Stream transport vs
meridional Ekman transport vs mid-ocean transports between the Bahamas and Canary Islands). We then update the findings
of Smeed et al. (2018) which reported a multiyear reduction in the AMOC strength using change point analysis. Based on the
00 RAPID observations and the recent findings at 45°N, we make preliminary investigations into the meridional coherence of the
AMOC transport variability between 26°N and 45°N, and the response at 26°N to the impulse forcing in 2013/15. Finally, we
place the latest AMOC transport record in context of the larger-scale Atlantic variability, its heat content and the AMV index.
These latest results show a possible recovery of the AMOC strength since its lowest point in 2009, but the short duration of
the record since 2014 precludes conclusive determination of the AMOC response to buoyancy forcing at this time.

05 2 Data

2.1 RAPID 26°N observations and transport calculations

10 The 14 years of observations at 26°N represent the most complete and longest record of the directly observed AMOC variability
currently available. The RAPID array (Fig. 1) spans the middle of the North Atlantic subtropical gyre close to the latitude at
which the ocean heat transport is maximum. Here the warm northward flowing waters of the western boundary current are
largely confined to the Florida Straits with a small but highly variable part flowing east of the Bahamas in the Antilles Current
(Meinen et al., 2019). Across the rest of the section there is a broad southward recirculation of the surface waters extending
across to the coast of Africa where seasonally varying upwelling gives rise to cooler water along the shelf edge. The deep
southward flow of the AMOC is predominantly close to the western boundary and transports two distinct water masses: one
15 centered around 1500 m depth, formed within the subpolar gyre, and often referred to as Upper North Atlantic Deep Water
(UNADW), and the other below 3000 m originating in the Nordic Seas and referred to as Lower North Atlantic Deep Water
(LNADW). Deeper still, Antarctic Bottom Water (AABW) flows northward in the western basin.

The objective of the RAPID array is to obtain a continuous and accurate record of the AMOC volume transport, and the
associated meridional heat and freshwater transports. Here we focus on the volume transport; updated analyses of the heat and
freshwater transports will be the subject of a separate study. There are three principal components to the measurements: (1)

Formatted: Space After: 5 pt

Deleted: document the period

Deleted: surface forcing to determine whether it is an anomalous period.

Deleted: surface-forced index of watermass transformation in the subpolar gyre, and a

Deleted: 45°N indicated

Deleted: (

Deleted: than 5-years) between the buoyancy forcing and the overturning strength (Desbruyères

Deleted: 45°N since about 2009.

Deleted: change point

Deleted: Guided by

Deleted: then

Deleted: The

Formatted: Space After: 5 pt

Formatted: Font color: Black

Deleted: .

Formatted: Font color: Black

Deleted: 26°N

Deleted: 3

Formatted: Font color: Black

Formatted: Normal, Border: Top: (No border), Bottom: (No border), Left: (No border), Right: (No border), Between : (No border), Tab stops: 7.96 cm, Centered + 15.92 cm, Right

the flow through the Florida Straits, the Florida Current, is monitored by a subsea cable calibrated by frequent hydrographic surveys (www.aoml.noaa.gov/phod/floridacurrent/), (2) the flow on the steep continental slope east of the Bahamas is measured by direct velocity measurements from an array of current meters referred to as the western boundary wedge (WBW), and (3) east of the WBW, geostrophic balance is used to estimate the flow from an array of dynamic height moorings. Instruments include, at present, 155 CTDs (conductivity-temperature-depth), 61 current meters, 3 ADCPs (acoustic Doppler current profilers), an additional 43 CTD-Os (CTDs with oxygen), 36 bottom pressure recorders (BPRs) and 4 PIES (pressure-inverted echo sounders). The dynamic height moorings are arranged in three sub-arrays: the western boundary array, the Mid-Atlantic Ridge (MAR) array and the eastern boundary array. The use of boundary moorings which sample at high frequency (hourly) enables high frequency (e.g. tidal and mesoscale) variability to be resolved and not aliased (Kanzow et al., 2009). In addition, the ageostrophic meridional Ekman transport is derived from the ERA5 reanalysis for zonal surface stress. A full description of the methodology for calculating the AMOC transports is given in McCarthy et al. (2015), and updated in the dataset release notes at https://www.rapid.ac.uk/rapidmoc/rapid_data/datadl.php.

2.2 AMOC transport at 45°N

In order to compare the RAPID AMOC observations to the wider Atlantic, we use an observational estimate of the AMOC at 45°N which uses a combination of satellite altimetry, reanalysis products and in situ ocean data (Desbruyères et al., 2019, after Mercier et al., 2015). Note, however, that the AMOC at 45°N is defined in density classes (AMOC_ρ). At 26°N, the transport variability is unlikely to be strongly different between the AMOC in depth-space and density-class as isopycnals across the broad expanse of the basin (6000km) are nearly flat. However, in the subpolar gyre, the overturning is defined in density coordinates (Pickart and Spall 2007; Mercier et al., 2015; Lozier et al., 2019) to better account for the dynamics of buoyancy redistribution in the ocean, which is also carried out by the horizontal gyre circulation. In the subpolar gyre, overturning is a measure of watermass transformation between the northward 'inflow' and southward 'outflow', irrespective of the depth at which it occurs. As the ad hoc reconstruction of the AMOC at 45°N is less constrained than the mooring-based RAPID estimates at 26°N, a comparison will be used to investigate their potential links.

2.3 Other data sets

The sea surface temperature (SST) product used here was the monthly average ERA5 reanalysis at 0.25° resolution (C3S, 2017) from 1979 to present. The winter (January to March) North Atlantic Oscillation (NAO) time series was calculated from the monthly mean NAO from the NOAA Climate prediction centre. The AMV is a measure of the low frequency variability in the Atlantic on multidecadal timescales, calculated from sea surface temperatures (SSTs) as a North Atlantic average, with the background tendency (Enfield et al., 2001) or background field (Trenberth and Shea, 2006) removed. Here, we use the definition following Sutton and Dong (2012) which is the normalized difference between the 10-year smooth Atlantic SST (equator to 65°N, 75°W to 7.5°W) and global mean SST which is close to that of Trenberth and Shea (2006). This definition contrasts from earlier definitions which averaged the North Atlantic SSTs and then detrended over the record. However,

Formatted: Font color: Black

Formatted: Font color: Black

Deleted: In addition the non-geostrophic

Formatted: Font color: Black

Formatted: Font: NimbusRomNo9L

Deleted: The AMOC at 45°N has been calculated using

Deleted: .

Deleted: .

Deleted: net

Deleted: The monthly average ocean heat content was calculated using temperature profiles from the EN4 v4.2.1 gridded 1° gridded dataset (Good et al., 2013).

Formatted: Space After: 5 pt

Deleted: JFM

Deleted: ¶

Deleted: 4¶

Formatted: Font color: Black

Formatted: Normal, Border: Top: (No border), Bottom: (No border), Left: (No border), Right: (No border), Between : (No border), Tab stops: 7.96 cm, Centered + 15.92 cm, Right

detrending is subject to the time period under consideration and does not allow for nonlinear variations in the time series of global SSTs (Frajka-Williams et al., 2017; Zhang et al., 2019).

80 We also use data from the GloSea5 global ocean and sea ice reanalysis (Blockley et al., 2014; Jackson et al., 2016), which uses
the NEMO GO5 ocean model with a nominal resolution of 0.25° and with 75 vertical layers (Megann et al., 2014). It assimilates
in-situ and satellite sea surface temperatures; sub-surface ocean profiles of temperature and salinity; sea ice concentration; and
sea level anomalies using the NEMOVAR v13 assimilation scheme (Waters et al., 2015). The experiment is described in more
85 detail in Jackson et al. (2016), with a more in-depth comparison to observations and other ocean reanalyses in Jackson et al
(2019).

3 Methods

3.1 Time series processing

The Florida Current transport is produced at daily resolution after a 3-day low-pass filter is applied. Individual instrument records at 26°N are either half-hourly or hourly, and filtered with a 2-day low pass filter to remove tides. Transports are then
90 calculated on a 12-hour grid, with a 10-day low-pass filter applied. Here the data are binned to 10-day time intervals before further analysis. The seasonal cycle is calculated by least-squares fitting an annual and semi-annual harmonic, with a fixed phase and amplitude over the full (2004-2018) record. McCarthy et al. (2015) find that the accuracy of the 10-day binned data is ±1.5 Sv, a figure that was corroborated by the model analysis of Sinha et al. (2018). The accuracy of the mean annual cycle derived from 18 years of data has been estimated using Monte-Carlo technique in which a normal distributed error with standard deviation 1.5 Sv is added to the monthly data. While the annual cycle appears to vary over the record, as noted in Calafat et al. (2018), further investigation of the annual cycle of transports is beyond the scope of the current investigation. Anomalies relative to the seasonal cycle are low-pass filtered using a 540-day Tukey filter.

Spectra are calculated using a Welch's overlapped segment averaging approach, with a Hamming taper and 50% overlap on the detrended, 10-day binned time series. In order to retain variability at low frequencies, while reducing noise at high
00 frequencies, we use three different window lengths following Kanzow et al. (2010).

For investigations into the relationship between the AMOC at 26°N and 45°N, we consider the geostrophic portion of the AMOC transports. i.e., at 26°N, we subtract the Ekman component from the total AMOC. This is because the Ekman component is independently forced at different latitudes and would not be anticipated to show low frequency coherence between latitudes. The AMOC transport at 45°N is computed without a contribution from surface Ekman transport. Both
05 records are then filtered with a 5-year lowpass Tukey filter.

Formatted: Space After: 5 pt

Moved (insertion) [1]

Deleted: 2014-2018) record.

Deleted: 3

Deleted: ..

Deleted: 5

Formatted: Font color: Black

Formatted: Normal, Border: Top: (No border), Bottom: (No border), Left: (No border), Right: (No border), Between : (No border), Tab stops: 7.96 cm, Centered + 15.92 cm, Right

3.2 Changepoint analysis

To analyse the variability of the AMOC transports, we use changepoint analysis on the 10-day total AMOC, minus Ekman (hereafter AMOC-Ekman) time series. The methodology is described in Beaulieu & Killick (2018) and is similar to that used in Smeed et al. (2018). A suite of eight models were fitted to the data, in which the short term variability is modelled by either random white-noise or a first order autocorrelation [AR(1)] process. The long-term variability is modelled as either a constant value, a linear trend, or one or more changepoints separating periods each linear with time. Combining all these possibilities for both the short-term and long-term variability leads to a total of eight models: (i) a constant mean with a white-noise background, 'Mean', (ii) a constant mean with first-order autocorrelation 'Mean+AR(1)', (iii) a linear trend 'Trend', (iv) a linear trend with first-order autocorrelation 'Trend+AR(1)', (v) multiple changepoints in the mean with a background of white-noise 'Mean+CP', (vi) multiple changepoints in the mean with first-order autocorrelation 'Mean+AR(1)+CP', (vii) multiple changepoints in the trend with white-noise 'Trend+CP', and (viii) multiple changepoints in the trend with first order autocorrelation 'Trend+AR(1)+CP'. For the models with changepoints, we find the number and locations using the pruned exact linear time algorithm (Killick et al., 2012), which performs an exact search considering all options for any possible number of changepoints and select the optimal number/location balancing the overall fit against the length of each segment. The most appropriate model is selected according to the Akaike Information Criterion (AIC). The AIC differences between each model included in the comparison and the model with the smallest AIC are also computed to assess plausibility of all models. As a rule of thumb, a difference larger than 10 indicates that there is essentially no support for a model given the data and the other models at play (Beaulieu & Killick, 2018). To verify sensitivity to the choice of information criterion, the Bayesian Information Criterion for each model is also computed. The changepoint analysis was conducted using the R package EnvCpt (Killick et al., 2018).

4 Results

4.1 Characterising the variability of the AMOC at 26°N

The AMOC volume transports are given in units of Sverdrups, where $1 \text{ Sv} = 10^6 \text{ m}^3 \text{ s}^{-1}$. To investigate the variability in the AMOC total and component transports, we calculate frequency spectra (Fig. 2). We only consider fluctuations with periods longer than 20 days as the method of calculating the AMOC transport assumes zero net meridional mass transport; this assumption is only valid on timescales longer than about 10-days (Kanzow et al., 2007). For periods shorter than about 60 days, Ekman transport dominates the variability of the AMOC; at other sub-annual periods, the variability is similar among all three components. Broad peaks in the spectra are found at both annual and semi-annual frequencies, particularly for the upper mid-ocean (UMO) transports, however on timescales shorter than 1 year, fluctuations in the UMO and Florida Current transports are anti-correlated (Frajka-Williams et al., 2016). This anti-correlation results in reduced power at the semi-annual

Formatted: Space After: 5 pt

Deleted: -

Deleted:

Deleted: The changepoint analysis was conducted using the R package EnvCpt (Killick et al., 2018).

Deleted: Methods

Formatted: Normal, Space After: 5 pt, Line spacing: single

Deleted: makes an assumption about the

Deleted: .

Deleted: anti-correlated,

Deleted: .

Deleted:) resulting

Deleted: a reduction of

Deleted: 6]

Formatted: Font color: Black

Formatted: Normal, Border: Top: (No border), Bottom: (No border), Left: (No border), Right: (No border), Between: (No border), Tab stops: 7.96 cm, Centered + 15.92 cm, Right

50 frequency in the total AMOC as compared to the UMO. At periods longer than a year, the AMOC variability is dominated by the UMO transport.

In view of the large and broad spectral peaks we have decomposed the time series into three parts: the seasonal cycle, an interannual signal, and the residual high frequency signal (Fig. 3). There is a substantial seasonal cycle with an amplitude of 2.0 ± 0.1 Sv and 0.7 ± 0.1 Sv (mean and standard error from Monte Carlo estimation) for the annual and semi-annual harmonic, explaining 11% and 2% of the variance, respectively. The residual timeseries, likewise, retains substantial variability with a range of 21.6 Sv and a standard deviation of 3.4 Sv. About 20% of the residual variance is associated with the estimated error of ± 1.5 Sv for the 10-day binned data. The large amplitude, sub-annual variability is a compelling reason why continuous, time-resolved in situ observations are required to firmly establish the mean value of the AMOC transports.

60 For the remainder of the paper, we focus on the low frequency (interannual) variability of the AMOC and component transports (Fig. 4). Both from the spectra and the time series in Fig. 4, it is clear that the low frequency variability in the total overturning transports is governed primarily by the mid-ocean transports, i.e., the upper mid-ocean component and the J_NADW layer. This is consistent with previous investigations into the AMOC variability, which showed smaller interannual variability in the Ekman and Florida Current transports than the mid-basin (Bahamas to Canary Islands). It is interesting to note, however, that a reduction in the Ekman transport closely follows the two minima in the UMO transport (2009 and 2012).

65 The low frequency changes in the AMOC are acyclic, and, based on data through 2012, were described using a linear trend by Smeed et al. (2014). However, the tendency of the time series through 2016 was not monotonic (Smeed et al., 2018), rendering a linear trend less useful at describing the observed variability. Instead, a changepoint analysis was used to fit a model to the total AMOC transport, concluding that for the record through 2016, the total AMOC transport variations were best described by two periods with constant mean values, separated by a single changepoint in 2008-2009 (Smeed et al., 2018). Here, we apply an updated version of the changepoint analysis to the AMOC-Ekman time series through 2018 (Fig. 5). This analysis also finds a changepoint in 2008 (Fig. 5b) in accord with the previous result.

70 Overall, these results are consistent with the previous analyses of the low frequency variability of the AMOC transport and its component parts. However, we note from the table of annual means (Table 1), that the mean in 2017/18 (calculated over the period 1 April 2017 - 31 March 2018) was 17.8 ± 1.4 Sv (mean \pm standard error, computed on the 10-day binned time series). The standard errors are large, due to substantial sub-annual fluctuations in the AMOC strength. The AMOC transport in the 2017/18 year (17.8 ± 1.4 Sv) is larger than the recent minimum in 2009/10 (13.5 ± 1.3 Sv) but this does not represent a return to the high AMOC transport values near the beginning of the observational record (2005/06, 20.9 ± 1.2 Sv). While the interannual time series appears to show a steadily, if weakly, increasing AMOC transport (Fig. 4a), this is not identified as the leading behaviour in the changepoint analysis and so is not yet a statistically significant increasing tendency.

Deleted: strength relative

Deleted: Sv

Deleted:

Deleted: 23.7

Formatted: Font: 12 pt

Deleted:

Deleted: lower North Atlantic Deep Water

Deleted: reductions

Deleted: following

Deleted:

Deleted: consistent

Deleted: , i.e. the geostrophic portion of the large-scale circulation

Deleted:

Deleted:

Deleted: confirms the existence of

Deleted: change point, now localising it around 2009-2010, but with constant mean values before and after

Deleted:)

Formatted: Space After: 5 pt

Deleted: .9

Deleted: deviation

Deleted:

Deleted: deviations

Deleted: This

Deleted: value in the year with the

Deleted: transports (

Deleted: ,

Deleted: 4.4 Sv) but still smaller than

Deleted: year with

Deleted: maximum

Deleted: 4.0

Deleted:

Deleted: 7

Formatted: Font color: Black

Formatted: Normal, Border: Top: (No border), Bottom: (No border), Left: (No border), Right: (No border), Between: (No border), Tab stops: 7.96 cm, Centered + 15.92 cm, Right

10

4.2 AMOC relationship between 26°N and 45°N

15

20

25

30

35

40

The 2013/14 and 2014/15 winters saw the return of deep convection in the Labrador Sea in two great impulse events (Yashayaev and Loder, 2016). These localised deep convection events are part of wider and longer-term intensification in subpolar water mass transformation that was at a minimum in 2005 (Desbruyères et al., 2019). Those changes have driven an overall intensification of the light-to-dense water mass transformation rates, sustaining a delayed (5-6 years) intensification of the AMOC at the southern exit of the subpolar gyre since 2010, as found in a recent observational analysis (Desbruyères et al., 2019). Building on previous studies, the arrival of such a signal at subtropical latitudes can be anticipated after 3-9 years, based on models (Johnson and Marshall, 2002; Zhang 2007) and observations (Molinari et al., 1998; van Sebille et al. 2011). Lagrangian studies have been used to identify when newly formed dense waters from the subpolar gyre reach the subtropics, with anomalies moving with the currents via advection (e.g., Bower et al., 2009; Zou et al., 2016; Jackson et al., 2016). However, transport time series can also adjust more rapidly through a fast boundary-wave mediated response of lower latitude AMOC variability to high latitudes forcing. Such a response can potentially be identified by lag correlation or coherence analysis of AMOC transport time series, rather than hydrographic anomalies. Based on the increase in subpolar watermass transformation peaking in 2013-2015 and various time lags between the subpolar-to-subtropical AMOC strength determined from numerical simulations, we would anticipate a sign of the increasing subtropical AMOC by 2018-2022. Determining the particular timing of the adjustment would provide critical groundtruth to meridional coherence investigations.

To investigate meridional coherence, we use the AMOC variations at 26°N and 45°N (Fig. 6a). We have removed the ageostrophic Ekman component to isolate AMOC - Ekman as the geostrophic part of the overturning. Ekman transports are forced independently at each latitude, while the geostrophic part of the overturning is the part of the signal that we would expect to show meridional coherence. The records are short, particularly the in situ observations at 26°N, for the filtering applied (5-years), but both latitudes show a decrease in the AMOC - Ekman over the 2004 - 2011 period of more than 3 Sv (45°N) and 2 Sv (26°N). This is followed by an increase at 45°N commencing around 2010-2011. Due to the length of the filter (5-years) and the relatively short duration of the in situ 26°N observations, we additionally use GloSea5 estimates at 26°N for a longer overlap period (Fig. 6a).

Comparing the AMOC-Ekman strength between altimetry/hydrography observations 45°N and GloSea5 estimates at 26°N, we find that they show similar timing of relative peaks (1996-1997, 2004-2005) and troughs (2000-2001, 2011, 2011-2013). The near coincidental occurrence of peaks and troughs is consistent with an expectation of some meridional coherence between latitudes. Since 2010, the AMOC at 45°N has been increasing. However, at 26°N the AMOC transport does not yet show a significant increase (see Section 3.2).

With the relatively short duration records and the absence of a clear impulse anomaly to track between latitudes, it is not yet possible to identify the timescale of adjustment between the subpolar and subtropical AMOC strength. It appears, however, from comparing the 45°N observational estimate of the AMOC and 26°N from GloSea5, that the adjustment timescale may be short (0-2 years). In contrast, within the GloSea5 reanalysis itself there was a mean lag of 7 years between a peak in Labrador

- Deleted: 4.2 Relationship to other latitudes [1]
- Formatted ... [3]
- Formatted ... [4]
- Deleted: Those localized [5]
- Formatted ... [5]
- Deleted: in air-sea interactions that occurred over the subpolar [6]
- Formatted ... [7]
- Deleted: that sustained [8]
- Formatted ... [8]
- Deleted: SPG [9]
- Formatted ... [9]
- Deleted: modelling [10]
- Formatted ... [10]
- Deleted: depending [11]
- Formatted ... [11]
- Deleted: on how waves or advection mediate that response [12]
- Formatted ... [13]
- Deleted: We note here that the recent results of Zou et al. ... [14]
- Formatted ... [15]
- Deleted: of UNADW in the subpolar gyre and that of LNADW [16]
- Formatted ... [17]
- Deleted: would be anticipated by 2017-2023. [18]
- Formatted ... [18]
- Deleted: Fig. 6a shows [19]
- Formatted ... [19]
- Deleted: 5-year low-pass filtered [20]
- Formatted ... [20]
- Deleted: , where both the RAPID observations and reanalysis [21]
- Formatted ... [22]
- Deleted: which are [23]
- Formatted ... [23]
- Deleted: , and [24]
- Formatted ... [24]
- Deleted: - [25]
- Formatted ... [25]
- Deleted: - [26]
- Formatted ... [26]
- Deleted: . [27]
- Formatted ... [27]
- Formatted ... [28]
- Deleted: AMOC-Ekman at 45°N slightly leads anomalies at 26°N [29]
- Formatted ... [30]
- Deleted: model studies that predict propagation from high [31]
- Formatted ... [32]
- Deleted: (Zang [33]
- Formatted ... [33]
- Deleted: ; Ortega et al., 2017). With these two time series [34]
- Formatted ... [34]
- Deleted: variability in [35]
- Formatted ... [35]
- Deleted: estimate of AMOC-Ekman [36]
- Deleted: 8 [37]
- Formatted ... [1]
- Formatted ... [2]

20 Sea density and the AMOC at 26°N (Jackson et al., 2016). This discrepancy is difficult to reconcile. While GloSea5 has been validated against the 26°N observations, there does not exist an equivalent long AMOC record in the subpolar gyre to verify GloSea5: the OSNAP estimate of the AMOC is too short (21 months) to verify interannual variability of reanalyses (Lozier et al., 2019) and the method used at 45°N with altimetry and gridded hydrography may be subject to errors particular in resolving higher frequency anomalies at the boundary.

25 It is further worth noting that the AMOC at 45°N is in density space, following the choice in Desbruyères et al. (2019); the AMOC_z at 45°N is in phase with the AMOC₀, but with lower amplitude (Desbruyères et al., 2019, Figure S4). In addition, the ratio of meridional heat transport to AMOC, a measure of how 'efficient' the overturning circulation is at fluxing heat, is greater at 26°N than 45°N (Johns et al., 2011; Desbruyères et al., 2019). This means that smaller amplitude fluctuations of the AMOC 26°N than 45°N may be associated with equivalent heat transport variability. More thorough investigations into depth- and zonal-distribution of changes at 26°N that accompany the subtle intensification of the overturning strength are pending. 30 These may enable a more conclusive determination of the arrival of the buoyancy-forced signals in the subtropical North Atlantic.

4.3 Ongoing changes in the wider Atlantic

35 To place the low frequency variability of the AMOC noted above in the wider Atlantic context, we consider large-scale variations in SST and atmospheric variability. On the one hand, the AMOC is anticipated to respond to wind- and buoyancy-forcing, and on the other, it drives heat transport and through it, heat content and SST changes. On multidecadal timescales, Gulev et al. (2013) provided observational evidence that in the mid-latitude North Atlantic and on timescales longer than 10 years, surface turbulent heat fluxes are indeed driven by the ocean and may force the atmosphere, whereas on shorter timescales the converse is true. Numerical simulations identified a driving role in the subtropical meridional heat transport for temperature tendencies in the subpolar North Atlantic (Moat et al., 2019). While the current record of in situ observations is too short to fully-investigate multi-decadal relationships, we can look more closely at the period of the observations and the longer records of SST to evaluate whether the observed variations in the Atlantic, as indexed by the AMV, follow the patterns predicted by the numerical simulations.

45 The AMV is a record of the multidecadal variations in the North Atlantic, based on SST (Fig. 6b). During the period prior to 2007/2008 the AMOC is generally in a positive state (Fig. 6a), which leads to greater than average northwards heat transport as the AMOC volume transport and meridional heat transport are proportional (Johns et al., 2011). This northward heat transport then leads to a warming North Atlantic, consistent with a positive AMV state (Fig 6b - from increased SST). After 2007/2008 the AMOC moves into a negative state with less than average northwards heat transport, which is followed by decreasing SST's and reducing AMV. Using a coupled climate model Moat et al., (2019) showed that on decadal time scales 50 changes the AMOC leads the AMV by about 5 years. There is evidence here to suggest that the AMV does not respond

Formatted: Font: Times New Roman
Deleted: is more markedly lower than at 45°N. It
Formatted: Font: Times New Roman

Formatted: Font: Times New Roman
Deleted: again
Formatted: Font: Times New Roman
Deleted: Desbruyères
Deleted:), but that

Formatted: Space After: 5 pt
Formatted: Font: Times New Roman
Formatted: Font: Times New Roman
Deleted: Desbruyères
Formatted: Font: Times New Roman
Formatted: Font: Times New Roman
Deleted: ,

Formatted: Font: Times New Roman
Deleted:
Formatted: Font: Times New Roman
Deleted:

Formatted: Font: Times New Roman
Formatted: Space After: 5 pt
Deleted: ocean heat content,
Deleted: ¶
Deleted: ,

Deleted: gyre
Deleted: ocean heat content and SSTs
Deleted: Since 1985, there was a steady increase in
Deleted: SSTs, peaking in 2008

Deleted: a decline. The full-depth ocean heat content (OHC) anomaly in the subpolar North Atlantic (80°W to 20°E, 45°N to 67°N) shows a similar pattern of change, indicating that while the AMV is a record of SSTs, it is indicative of subsurface temperatures as well. From e.g.,

Deleted: .
Deleted: in a 1/4 degree ocean model, we anticipate that
Deleted: in the AMOC

Deleted: ¶
Formatted: Font color: Black

Formatted: Normal, Border: Top: (No border), Bottom: (No border), Left: (No border), Right: (No border), Between : (No border), Tab stops: 7.96 cm, Centered + 15.92 cm, Right

instantaneously with the AMOC and the AMOC may lead the AMV. However, the length of the AMOC at 26°N is currently too short for the lagged correlations to be statistically significant.

The long-timescale fluctuations in the AMV contrast with atmospheric variability, as measured by the North Atlantic Oscillation index (NAO), which tends to vary on shorter 3-5 year timescales. The low-passed NAO was in a positive state with a maximum around 1990 and declining to near zero in 2005. During this period AMOC was in a positive state moving more than average heat northwards (GloSea5, Fig 6a). As the NAO declines into a -ve state there is a reduction in the surface heat loss in the subpolar region of the North Atlantic, which is followed by a reducing AMOC strength. Since 2010 the NAO is recovering from a minimum and moving towards a NAO+ state, resulting in enhanced heat loss in the subpolar North Atlantic and strengthening the AMOC. Given the lag between the AMOC and AMV described above we would anticipate an increase in the AMV with increasing AMOC, which is consistent with the hypothesis illustrated in Sutton et al. (2018).

From this large-scale view of the Atlantic, we can conclude that the observed AMOC variability, SST variability (measured by the AMV) and atmospheric forcing (measured by the NAO) are consistent with various numerical studies (Moat et al., 2019; Sutton et al., 2018). A positive NAO period is associated with stronger heat loss from the subpolar North Atlantic, providing buoyancy forcing to strengthen the AMOC. And a strong AMOC will flux more heat northward leading to a warmer North Atlantic (more positive AMV). While the recent decade offers a change in state of the Atlantic (AMV) as well as anomalous buoyancy forcing in subpolar North Atlantic (2013-2015), the time series of directly-measured AMOC variability at 26N is not yet long enough to conclusively test the mechanisms linking buoyancy forcing to circulation change, and leading to changes in ocean heat content. A more complete diagnosis of the short-term heat budget (2014-2020) and the relative contributions of ocean transports and surface fluxes is beyond the scope of this paper, but currently underway.

5 Conclusions

From the nearly 15-year long record of the AMOC variability at 26°N, we can characterise the transports as highly variable on all timescales, with high frequency variability (shorter than 60 days) dominated by rapid fluctuations in the zonal winds across 26°N, seasonal cycles contributed to by the UMO transport between the Bahamas and Canary Islands, and low frequency variability dominated by the UMO transports and mirrored in the LNADW layer (3000-5000m). This is in agreement with previous investigations into the seasonal cycle (Kanzow et al., 2010; Duchez et al., 2014), high frequency variability (Moat et al., 2016) and interannual variability (McCarthy et al., 2012), compensation between components (Kanzow et al., 2007; Frajka-Williams et al., 2016). Using the full duration of the record, we further investigate the tendency in the record finding that the decline previously identified as a trend (Smeed et al., 2014) and as a changepoint between two periods with a higher and lower mean (Smeed et al. 2018) has not yet reversed. While the lowpass filtered AMOC time series appears to show an increasing tendency since 2009 (Fig. 3c), this increase is not statistically significant.

The recent intense heat loss in the subpolar North Atlantic (2013-2015) and the extension of the RAPID record through 2018, motivated an investigation into when and how the RAPID transports would respond to buoyancy forcing in the subpolar gyre

Deleted: by about 4 years. The

Formatted: Space After: 5 pt

Deleted: is an indicator of the atmospheric state. The lowpassed

Deleted: in 1991

Deleted:

Deleted: 2011. It is out-of-phase with the AMV and ocean heat content. The relationship between NAO, AMOC at 26°N, AMV and ocean heat content is consistent with the pattern described

Formatted: Highlight

Deleted:

Deleted: Comparing the large-scale climate indices with the transport estimates at two latitudes, we can evaluate the relationship between heat transported by the ocean and the temperature changes in the Atlantic. After the NAO maximum around 1990, the AMOC reaches a peak (around 1996 at 45°N and 1997 in the GloSea5 estimate (Jackson et al., 2019)), followed by an increase in the AMV to a maximum in 2007, and a high anomaly in full depth ocean heat content between 2006-2012, with a peak in 2012. As the AMOC transports decreased, relative to these previous strong values, the

Formatted: Space After: 5 pt

Deleted: Lower North Atlantic Deep Water

Deleted: .

Deleted: .

Deleted: .

Deleted: .

Deleted: .

Deleted: .

Deleted: .

Deleted:), and interannual and longer term variability (

Moved up [1]: McCarthy et al.

Formatted: Font: Bold

Deleted: 2012,

Deleted: 2014,

Deleted:). One remarkable finding from these previous studies

Deleted: strength in

Deleted: -10 (Roberts et al. 2013), calling into question the ...

Deleted: driven by buoyancy forcing at high latitudes (Lozier, ...)

Formatted: Font: Bold

Deleted: whether

Deleted: when

Deleted: 10°

Formatted: Font color: Black

Formatted ... [36]

forcing. In situ estimates of the overturning at 45°N indicate that at 45°N, near the southern boundary of the subpolar gyre, the overturning strength is already intensifying following sustained buoyancy forcing in the subpolar gyre (Desbruyères et al. 2019). Comparing the transport variability at 26°N and 45°N, we show some indication of a potential lead-lag relationship (45°N leading changes at 26°N by 0-2 years) in the AMOC-Ekman transports, but with stronger amplitude variations at 45°N. As yet, however, the available AMOC time series at 26°N does not show a statistically significant increase since the low period in 2010 (Fig 5).

In addition to the AMOC responding to subpolar changes, it is anticipated to cause change in the northern North Atlantic through changes in the meridional heat transport of the AMOC. The phase-relationship identified in the modelling study of Moat et al. (2019) relies on identifying periods where the AMOC is increasing or decreasing, or where it is positive vs negative (corresponding to increasing or decreasing accumulated northward heat transport). While the in situ record at 26°N is too short to conclusively determine the lag, a comparison between model reanalysis (GloSea5) AMOC at 26°N and the AMOC at 45°N supports this timing. Using these longer records, we find that the changes in the AMOC strength are consistent with an ocean role in driving variations in North Atlantic temperatures, but a more complete heat budget analysis is under investigation for a conclusive determination of the relative importance of ocean transports vs surface forcing.

The transport time series at 26°N in the Atlantic of the large-scale ocean circulation has yielded new insights into the variability of the overturning circulation (Srokosz and Bryden, 2015). The results here extend our knowledge of the AMOC variability through 2018, finding that the AMOC is marginally stronger in the period 2014-2018 than the preceding period (2009-2014) using a changepoint analysis. However, the lead-lag relationships between the AMOC at two latitudes (26N and 45N) cannot be conclusively determined. Additionally, the AMOC at 26N does not yet appear to be responding to the intense buoyancy loss in the subpolar gyre in 2013-2015. Based on the findings in Desbruyères et al. (2019), that the AMOC at 45°N lags basin-wide surface-forced transformation in the subpolar gyre by 5 years, and the tentative 0-2 year lag from the AMOC at 45°N to the AMOC at 26°N, we would anticipate an intensification in the overturning strength at 26°N in response to the 2013-15 forcing by 2018-2022, and may become apparent in the next recovery of the RAPID observations.

Data availability

The RAPID-MOCHA-WBTS time series (Smeed et al., 2019) is available at <http://www.rapid.ac.uk/rapidmoc>. ERA5 sea surface temperature (SST) is available via <https://www.ecmwf.int/en/forecasts/datasets/reanalysis-datasets/era5>. The GloSea5 time series is available from (Jackson et al., 2019). The 45°N time series of Desbruyères et al., (2019) is available from the author on request.

Deleted: this latitude

Deleted: Given that the results at 45°N follow the basin-wide surface-forced transformation in the subpolar gyre by 5 years, and the 0-2 years further lag to 26°N, we would anticipate an intensification in the overturning strength at 26°N in response to the 2013-15 forcing by 2019-2021. The length of the records collected to date are somewhat short, given the smoothing applied (5 years), and so determination of a lead-lag relationship through lagged correlation cannot provide significance. Instead, we have relied on a more speculative identification of peaks and troughs in the time series.

Formatted: Font: Bold

Deleted: at 26°N

Deleted: the heat transport variability at 26°N, particularly on longer timescales,

Deleted: lead to

Deleted: subpolar North Atlantic and broader Atlantic as a whole.

Deleted: With the record at hand, it is difficult to determine a 'reference period' around which to define an anomaly. Instead we note that the phased relationship with high values of the AMOC strength at 26°N (GloSea5 reanalysis) and 45°N occur during a period when the AMV is increasing (North Atlantic is warming), while the change in tendency of the AMV occurs when the AMOC values are low.

Moved down [2]: The transport time series at 26°N in the Atlantic of the large-scale ocean circulation has yielded new insights into the variability of the overturning circulation (Srokosz and Bryden, 2015).

Deleted: The results here extend our understanding of the AMOC variability through 2018 and investigate whether the recent strong buoyancy forcing in the subpolar gyre (2013-2015) is apparent yet in the transports at 26°N. We have concluded that the AMOC appears to be marginally stronger in the period 2014-2018 than the preceding period (2009-2014) and that this increase began roughly 0-2 years following the observed increase at 45°N.

Moved (insertion) [2]

Formatted: Font: Times New Roman

Formatted: Font: Times New Roman

Deleted: <http://www.rapid.ac.uk/rapidmoc>, ERA5 sea surface temperature (SST) is available via <https://www.ecmwf.int/en/forecasts/datasets/reanalysis-datasets/era5>. The EN4 profiles used to calculate the ocean heat content are available via ... [42]

Formatted: Font: Times New Roman

Formatted: Font: Times New Roman

Formatted: Font: Times New Roman

Formatted: Font: Times New Roman

Deleted: 11

Formatted: Font color: Black

Formatted ... [41]

Author Contributions

EFW, DAS, BIM, CB, DD wrote the manuscript with input from all authors. BIM, DR, DD, DAS, HLB contributed to the transport calculations. DAS, CB, BIM, EFW, ASF, [LCJ](#) performed the analysis. WEJ, DV, MOB, BIM, DAS, DR, EFW, HLB contributed to the data collection.

Competing interests

The authors declare they have no conflict of interest.

Acknowledgements

This research was supported by grants from the UK Natural Environment Research Council for the RAPID-AMOC program and the ACSIS program (NE/N018044/1), by the U.S. National Science Foundation (grant 1332978), by the U.S. National Oceanic and Atmospheric Administration (NOAA) Climate Program Office (100007298), and by the U.S. NOAA Atlantic Oceanographic and Meteorological Laboratory. The authors thank the many officers, crews, and technicians who helped to collect these data.

References

Barber, D. C., Dyke, A., Hillaire-Marcel, C., Jennings, A. E., Andrews, J. T., Kerwin, M. W., Bilodeau, F., McNeely, R., Southon, J., Morehead, M. D. and Gagnon, J.-M.: Forcing of the cold event of 8,200 years ago by catastrophic drainage of Laurentide lakes, *Nature*, 400, 344-348, DOI:10.1038/22504, 1999.

Beaulieu, C. and Killick, R.: Distinguishing trends and shifts from memory in climate data Distinguishing trends and shifts from memory in climate data, *J. of Climate*, 31, 9519-9543. DOI:10.1175/jcli-d-17-0863.1, 2018.

[Blockley, E. W., Martin, M. J., McLaren, A. J., Ryan, A. G., Waters, J., Lea, D. J., Mirouze, I., Peterson, K. A., Sellar, A., and Storkey, D.: Recent development of the Met Office operational ocean forecasting system: an overview and assessment of the new Global FOAM forecasts, *Geosci. Model Dev.*, 7, 2613–2638, 2014.](#)

[Bower, A. S., Lozier, M. S., Gary, S. F., and Böning, C. W.: Interior pathways of the North Atlantic Meridional Overturning Circulation, *Nature*, 459, doi:10.1038/nature07979, 2009.](#)

[Bryden, H. L., Johns, W. E., King, B. A., McCarthy, G. A., McDonagh, E. L., Moat, B. I., Smeed, D. A.: Reduction in ocean heat transport at 26°N since 2008 cools the eastern subpolar gyre of the North Atlantic Ocean, *J. of Climate*, 33, 1677-1689. DOI: 10.1175/JCLI-D-19-0323.1, 2020.](#)

Deleted:

Formatted: Space After: 5 pt

Deleted: :

Deleted: :9519-9543. DOI:10.1175/jcli-d-17-0863.1.

Moved (insertion) [3]

Moved (insertion) [4]

Deleted: 12

Formatted: Font color: Black

Formatted: Normal, Border: Top: (No border), Bottom: (No border), Left: (No border), Right: (No border), Between : (No border), Tab stops: 7.96 cm, Centered + 15.92 cm, Right

80 Calafat F. M., Wahl, T., Lindsten, F., Williams, J. and Frajka-Williams, E.: Coherent modulation of the sea-level annual cycle
in the United States by Atlantic Rossby waves, *Nat. Comm.*, 9, 2571, DOI:10.1038/s41467-018-04898-y, 2018.

Formatted: Space After: 5 pt

Deleted: Comm., 9:2571, DOI:10.1038/s41467-018-04898-y, 2018.

Copernicus Climate Change Service (C3S) (2017): ERA5: Fifth generation of ECMWF atmospheric reanalyses of the global climate. Copernicus Climate Change Service Climate Data Store (CDS), 2019.

85 Cunningham, S. A., Kanzow T. O., Rayner D., Barringer M. O., Johns W. E., Marotzke J., Longworth H. R., Grant E. M.,
Hirschi J. J.-M., Beal L. M., Meinen C. S. and Bryden H. L.: Temporal variability of the Atlantic Meridional Overturning
Circulation at 26.5°N, *Science*, 317, 935-938, DOI:10.1126/science.1141304, 2007.

Deleted: :

Delworth, T. L. and Mann, M. E.: Observed and simulated multidecadal variability in the Northern Hemisphere, *Clim. Dyn.*,
16, 661–676, DOI:10.1007/s003820000075, 2000.

Deleted: :10.1007/s003820000075, 2000.

90 Desbruyères, D. G., Mercier, H., Maze, G. and Danialt, N.: Surface predictor of overturning circulation and heat content
change in the subpolar North Atlantic, *Ocean Science*, 15, 809–817, DOI:10.5194/os-15-809-2019, 2019.

Duchez, A., Frajka-Williams, E., Castro, N., Hirschi, J. and Coward, A.: Seasonal to interannual variability in density around
the Canary Islands and their influence on the Atlantic meridional overturning circulation at 26°N, *J. of Geophys. Res., Oceans*,
119, 1843-1860, DOI:10.1002/2013JC009416, 2014.

Deleted: :

Deleted: :

95 Duchez, A., Frajka-Williams, E., Josey, S. A., Evans, D. G., Grist, J. P., Marsh, R., McCarthy, G. D., Sinha, B., Berry, D. I.
and Hirschi, J. J.-M.: Drivers of exceptionally cold North Atlantic Ocean temperatures and their link to the 2015 European
heat wave, *Environ. Res. Lett.*, 11, DOI: 10.1088/1748-9326/11/7/074004, 2016.

Enfield, D. B., Mestas-Nunez, A. M. and Trimble, P. J.: The Atlantic Multidecadal Oscillation and its relationship to rainfall
and river flows in the continental U.S., *Geophys. Res. Lett.*, 28, 2077–2080, DOI:10.1029/2000GL012745, 2001.

Deleted: :

00 Frajka-Williams, E., Meinen, C.S., Johns, W.E., Smeed, D.A., Duchez, A., Lawrence, A.J., Cuthbertson, D.A., McCarthy,
G.D., Bryden, H.L., Baringer, M.O., Moat, B.I. and Rayner, D.: Compensation between meridional flow components of the
Atlantic MOC at 26°N, *Ocean Science*, 12, 481-493, DOI:10.5194/os-12-481-2016, 2016.

Deleted: :481-493, DOI:10.5194/os-12-481-2016,

Frajka-Williams, E., Beaulieu, C. and Duchez, A.: Emerging negative Atlantic Multidecadal Oscillation in spite of warm
subtropics, *Scientific Reports*, 7:11224, DOI:10.1038/s41598-017-11046-x, 2017.

Deleted: :10.1038/s41598-017-11046-x, 2017.

05 Frajka-Williams, E., Anson, I. J., Baehr, J., Bryden, H. L., Chidichimo, M. P., Cunningham, S. A., Danabasoglu, G., Dong,
S., Donohue, K. A., Elipot, S., Heimbach, P., Holliday, N. P., Hummels, R., Jackson, L. C., Karstensen, J., Lankhorst, M.,
Bras, I. A. L., Lozier, M. S., McDonagh, E. L., Meinen, C. S., Mercier, H., Moat, B. I., Perez, R. C., Piecuch, C. G., Rhein,
M., Srokosz, M. A., Trenberth, K. E., Bacon, S., Forget, G., Goni, G., Kieke, D., Koelling, J., Lamont, T., McCarthy, G. D.,
Mertens, C., Send, U., Smeed, D. A., Speich, S., van den Berg, M., Volkov, D. and Wilson, C.: OceanObs19: Atlantic
meridional overturning circulation: Observed transports and variability, *Frontiers in Marine Science*, 6:260,
10 DOI:10.3389/fmars.2019.00260, 2019.

Deleted: :10.3389/fmars.2019.00260, 2019.

Moved down [5]: Ganopolski, A. and Rahmstorf, S.:

Deleted: Rapid changes of glacial climate simulated in a coupled climate model, *Nature*, 409:153–158, DOI:10.1038/35051500, 2001

Deleted: 13*

Formatted: Font color: Black

Formatted: Normal, Border: Top: (No border), Bottom: (No border), Left: (No border), Right: (No border), Between : (No border), Tab stops: 7.96 cm, Centered + 15.92 cm, Right

25 [Ganopolski, A. and Rahmstorf, S.: Rapid changes of glacial climate simulated in a coupled climate model, Nature, 409, 153–158, DOI:10.1038/35051500, 2001.](#)

Moved (insertion) [5]

Deleted: Good, S. A

[Gulev, S.K., Latif M., Keenlyside N., Park, W. and Koltermann, K. P.: North Atlantic Ocean control on surface heat flux on multidecadal timescales, Nature, 499, 464–467, DOI:10.1038/nature12268, 2013.](#)

Moved up [3]: , Martin, M.

Formatted: Space After: 5 pt

Deleted: J. and Rayner, N. A.: EN4: quality controlled ocean temperature and salinity profiles and monthly objective analyses with uncertainty estimates, J. of

Moved down [6]: Geophys.

Deleted: Res.: Oceans, 118:6704-6716, DOI:10.1002/2013JC009067, 2013.

Deleted: :

30 IPCC: Observations: Ocean, in: Climate Change 2013: The Physical Science Basis. Contribution of Working Group I to the Fifth Assessment Report of the Intergovernmental Panel on Climate Change, edited by Stocker, T. F., Qin, D., Plattner, G.-K., Tignor, M., Allen, S., Boschung, J., Nauels, A., Xia, Y., Bex, V., and Midgley, P., p. 1535pp, Cambridge University Press, Cambridge, United Kingdom, DOI:10.1017/CBO9781107415324, 2013.

[Jackson, L. C., Peterson, K. A., Roberts, C. D., and Wood, R. A.: Recent slowing of Atlantic overturning circulation as a recovery from earlier strengthening, Nat. Geosci., 9, 518–522, 2016.](#)

Formatted: Space After: 5 pt

35 [Jackson J. C., Dubois C., Forget G., Haines K., Harrison M., Iovino D., Kohl A., Mignac D., Mashina S., Peterson K. A., Piecuch C. G., Roberts C., Robson J., Storto A., Toyoda T., Valdivieso M., Wilson C., Wang Y. and Zuo, H.: The mean state and variability of the north Atlantic circulation: a perspective from ocean reanalyses, J. of Geophys. Res., Oceans, 124, DOI:10.1029/2019JC015210, 2019.](#)

Deleted: :

Deleted: 134

40 [Johns W. E., Baringer, M. O., Beal, L. M., Cunningham, S. A., Kanzow, T., Bryden, H. L., Hirschi, J. J.-M., Marotzke, J., Meinen, C. S., Shaw, B. and Curry, R.: Continuous, Array-Based Estimates of Atlantic Ocean Heat Transport at 26.5°N, J. of Climate, 24, 2429–2449, DOI: 10.1175/2010JCLI3997.1, 2011.](#)

Deleted: :

[Johnson, H. L. and Marshall, D. P.: A theory for the surface Atlantic response to thermohaline variability, J. Phys. Oceanogr., 32, 1121–1132, DOI: 10.1175/1520-0485\(2002\)032<1121:ATFTSA>2.0.CO;2, 2002.](#)

Deleted: :

45 [Josey S A., Hirschi, J. J.-M., Sinha, B., Duchez, A., Grist, J. P. and Marsh, R.: The Recent Atlantic Cold Anomaly: Causes, Consequences, and Related Phenomena, Ann. Rev. Mar. Sci., 10, 475–501, DOI:10.1146/annurev-marine-121916-063102, 2018.](#)

Deleted: :10.1146/annurev-marine-121916-063102.

[Kanzow, T., Cunningham, S. A., Rayner, D., Hirschi, J. J.-M., Johns, W. E., Baringer, M. O., Bryden, H. L., Beal, L. M., Meinen, C. S. and Marotzke, J.: Observed flow compensation associated with the MOC at 26.5°N in the Atlantic, Science, 317, 938–941, DOI:10.1126/science.1141293, 2007.](#)

Deleted: :

50 [Kanzow T., Johnson, H., Marshall, D., Cunningham, S. A., Hirschi J. J.-M., Mujahid A., Bryden H. L., Johns, W. E.: Basin-wide integrated volume transports in an eddy-filled ocean, Journal of Physical Oceanography, 39, 3091–3110, doi:10.1175/2009JPO4185.1](#)

Formatted: Space After: 5 pt

Moved (insertion) [7]

Deleted: :

Deleted: 14

Formatted: Font color: Black

Formatted: Normal, Border: Top: (No border), Bottom: (No border), Left: (No border), Right: (No border), Between : (No border), Tab stops: 7.96 cm, Centered + 15.92 cm, Right

Killick, R., Beaulieu, C., Taylor, S. and Hurlait, H.: Envcp: Detection of structural changes in climate and environment time series (Version version 1.1.1). CRAN. Retrieved from <https://CRAN.R-project.org/package=EnvCpt>, 2018.

Deleted: Retrieved from <https://CRAN.R-project.org/package=EnvCpt>.

Lozier, M.S.: Deconstructing the Conveyor Belt, *Science*, 328, 1507-1511, DOI:10.1126/science.1189250, 2010.

Deleted: :

Lozier, M. S., Li, F., Bacon, S., Bahr, F., Bower, A. S., Cunningham, S. A., de Jong, M. F., de Steur, L., de Young, B., Fischer, J., Gary, S. F., Greenan, B. J. W., Holliday, N. P., Houk, A., Houpert, L., Inall, M. E., Johns, W. E., Johnson, H. L., Johnson, C., Karstensen, J., Koman, G., Le Bras, I. A., Lin, X., Mackay, N., Marshall, D. P., Mercier, H., Oltmanns, M., Pickart, R. S., Ramsey, A. L., Rayner, D., Straneo, F., Thierry, V., Torres, D. J., Williams, R. G., Wilson, C., Yang, J., Yashayaev, I. and Zhao, J.: A Sea change in our view of overturning in the subpolar North Atlantic, *Science*, 363, 516–521, DOI:10.1126/science.aau6592, 2019.

Deleted: :

Deleted: :10.1126/science.aau6592.

Formatted: Font: Not Italic, Font color: Auto

Mercier, H., Lherminier, P., Sarajanov, A., Gaillard, F., Daniault, N., Desbruyères, D. G., Falina, A., Ferron, B., Gourcuff, C., Huck, T. and Thierry, V.: Variability of the meridional circulation at the Greenland-Portugal OVIDE section from 1993 to 2010, *Prog. in Oceanogr.*, 132, 250-261, DOI:10.1016/j.pocean.2013.11.001, 2015.

Deleted: :

McCarthy, G., Frajka-Williams, E., Johns, W. E., Baringer, M. O., Meinen, C. S., Bryden, H. L., Rayner, D., Duchez, A., Roberts, C. D. and Cunningham, S. A.: Observed Interannual Variability of the Atlantic Meridional Overturning Circulation at 26.5°N, *Geophys. Res. Lett.*, 39:L19609, <https://doi.org/10.1029/2012GL052933>, 2012.

Deleted: <https://doi.org/10.1029/2012GL052933>, 2012.

McCarthy, G. D., Smeed, D. A., Johns, W. E., Frajka-Williams, E., Moat, B. I., Rayner, D., Baringer, M. O., Meinen, C. S. and Bryden, H. L.: Measuring the Atlantic meridional overturning circulation at 26°N, *Prog. in Oceanogr.*, 130:91–111, DOI:10.1016/j.pocean.2014.10.006, 2015.

Deleted: :10.1016/j.pocean.2014.10.006.

Megann, A. P., Storkey, D., Alksenov, Y., Alderson, S., Calvert, D., Graham, T., Hyder, P., Siddorn, J., and Sinha, B.: GO 5.0: The joint NERC–Met Office NEMO global ocean model for use in coupled and forced applications, *Geotech. Model Dev.*, 7, 1069–1092, 2014.

Meinen, C. S., W. E. Johns, B. I. Moat, R. H. Smith, E. Johns, D. Rayner, E. Frajka-Williams, R. F. Garcia, and S. L. Garzoli: Structure and variability of the Antilles Current at 26.5°N, *J. Geophys. Res. Oceans*, 124, 3700-3723, doi:10.1029/2018JC014836, 2019.

Moved (insertion) [8]

Moved (insertion) [6]

Moat, B. I., Josey, S. A., Sinha, B., Blaker, A. T., Smeed, D. A., McCarthy, G., Johns, W. E., Hirschi, J. J.-M., Frajka-Williams, E., Rayner, D., Duchez, A. and Coward, A.C.: Major variations in subtropical North Atlantic heat transport at short (5 day) timescales and their causes, *J. of Geophys. Res. Oceans*, 121, 3237-3249, DOI:10.1002/2016JC011660, 2016.

Formatted: Space After: 5 pt

Deleted: .:

Deleted: (5):

Deleted: :10.1002/2016JC011660.

Deleted: (18):

Deleted: :10.1175/JCLI-D-18-0709.1.

Moat, B. I., Sinha, B., Josey, S. A., Robson, J., Ortega, P., Sévellec, F., Holliday, N. P., McCarthy, G. D., New, A. L. and Hirschi, J. J.-M.: Insights into decadal North Atlantic sea surface temperature and ocean heat content variability from an eddy-permitting coupled climate model, *J. of Climate*, 32, 6137-6161, DOI:10.1175/JCLI-D-18-0709.1, 2019.

Deleted: 15*

Formatted: Font color: Black

Formatted: Normal, Border: Top: (No border), Bottom: (No border), Left: (No border), Right: (No border), Between: (No border), Tab stops: 7.96 cm, Centered + 15.92 cm, Right

15 [Molinari, R. L., Fine R. A., Wilson W. D., Curry R. G., Abell, J., and McCartney, M. S.: The arrival of recently formed Labrador Sea Water in the Deep Western Boundary Current at 26.5°N, Geophys. Res. Lett., 25, 2249–2252, doi:10.1029/98GL01853, 1998.](#)

Moved (insertion) [9]

Ortega, P., Robson, J., Sutton, R.T. and Andrews M. B.: Mechanisms of decadal variability in the Labrador Sea and the wider North Atlantic in a high-resolution climate model, Clim. Dyn., 49:2625, DOI:10.1007/s00382-016-3467-y, 2017.

Formatted: Space After: 5 pt

Deleted: :10.1007/s00382-016-3467-y,

20 [Pickart, R. S. and Spall, M. A.: Impact of Labrador Sea convection on the North Atlantic Meridional Overturning circulation, J. of Physical Oceanogr., 37, 2207-2227, DOI:10.1175/JPO3178.1, 2007.](#)

Moved up [4]: L.,

Deleted: Østerhus, S., Woodgate, R., Valdimarsson, H., Turrell, B., de Stuur,

Deleted: Quadfasel, D., Olsen, S. M., Moritz, M., Lee, C. M., Larsen, K. M., Jónsson,

Moved up [8]: S.,

Deleted: Johnson, C., Jochumsen, K., Hansen, B., Curry, B

Roberts, C. D., Waters, J., Peterson, K. A., Palmer, M., McCarthy, G. D., Frajka-Williams, E., Haines, K., Lea, D. J., Martin, M. J., Storkey, D., Blockley, E. W. and Zuo, H.: Atmosphere drives observed interannual variability of the Atlantic meridional overturning circulation at 26.5°N, Geophys. Res. Lett., 40, 5164-5170, DOI: 10.1002/grl.50930, 2013.

Moved up [7]: ., Cunningham, S.

Deleted: and Berx B.: Arctic Mediterranean exchanges: a consistent volume budget and trends in transports from two decades of observations, Ocean Science, 15:379-399, DOI:10.5194/os-15-379-2019, 2019. ↑

Deleted: :

Deleted: :

Deleted: :

Formatted: Font: Not Italic, Font color: Auto

Formatted: Space After: 5 pt

Deleted:

Deleted: :29-38, <https://doi.org/10.5194/os-10-29-2014>,

Deleted: :

25 [Sinha, B., Smeed, D. A., McCarthy, G., Moat, B. I., Josey, S. A., Hirschi, J. J.-M., Frajka-Williams, E., Blaker, A. T., Rayner, D., Madec, G.: The accuracy of estimates of the overturning circulation from basin-wide mooring arrays, Progress in Oceanography, 160, 101-123, <https://doi.org/10.1016/j.pocean.2017.12.001>, 2018.](#)

Smeed, D. A., McCarthy, G., Cunningham, S. A., Frajka-Williams, E., Rayner, D., Johns, W. E., Meinen, C. S., Baringer, M.O., Moat, B. I., Duchez, A. and Bryden, H. L.: Observed decline of the Atlantic Meridional Overturning Circulation 2004–2012, Ocean Science, 10, 29-38, <https://doi.org/10.5194/os-10-29-2014>, 2014.

30 Smeed, D. A., Josey, S., Johns, W., Moat, B., Frajka-Williams, E., Rayner, D., Meinen, C., Baringer, M., Bryden, H. and McCarthy, G.: The North Atlantic Ocean is in a state of reduced overturning, Geophys. Res. Lett., 45, 1527–1533, DOI:10.1002/2017GL076350, 2018.

35 Smeed D., Moat B. I., Rayner D., Johns W. E., Baringer M. O., Volkov D. L. and Frajka-Williams, E.: Atlantic meridional overturning circulation observed by the RAPID-MOCHA-WBTS (RAPID-Meridional Overturning Circulation and Heatflux Array-Western Boundary Time Series) array at 26°N from 2004 to 2018. British Oceanographic Data Centre, National Oceanography Centre, NERC, UK. doi:10/c72s, 2019.

40 Srokosz, M., Baringer, M., Bryden, H., Cunningham, S., Delworth, T., Lozier, S., Marotzke, J. and Sutton, R.: Past, present and future changes in the Atlantic meridional overturning circulation, Bull. Amer. Meteorol. Soc., 93:1663–1676. DOI:10.1175/BAMS-D-11-00151.1, 2012.

Srokosz, M., Baringer, M., Bryden, H., Cunningham, S., Delworth, T., Lozier, S., Marotzke, J., Sutton, R.: Past, Present, and Future Changes in the Atlantic Meridional Overturning Circulation, Bulletin of the American Meteorological Society, 93, 1663-1676, <https://doi.org/10.1175/BAMS-D-11-00151.1>, 2012.

Deleted: 16

Formatted: Font color: Black

Formatted: Normal, Border: Top: (No border), Bottom: (No border), Left: (No border), Right: (No border), Between : (No border), Tab stops: 7.96 cm, Centered + 15.92 cm, Right

65 [Srokosz, M. A. and Bryden, H. L.:](#) Observing the Atlantic Meridional Overturning Circulation yields a decade of inevitable surprises, *Science*, 348, DOI:[10.1126/science.1255575](#), 2015.

[Sutton, R. T. and Dong, B.:](#) Atlantic Ocean influence on a shift in European climate in the 1990s, *Nature Geosci.*, 5, 788–792, DOI:[10.1038/ngeo1595](#), 2012.

Sutton, R. T., McCarthy, G. D., Robson, J., Sinha, B., Archibald, A. and Gray, L.J.: Atlantic multi-decadal variability and the UK ACSIS programme, *Bull. Amer. Meteorol. Soc.*, 99:415–425, DOI:[10.1175/BAMS-D-16-0266.1](#), 2018.

Trenberth, K. E. and Shea, D. J.: Atlantic hurricanes and natural variability in 2005, *Geophys. Res. Lett.*, 33:L12704, DOI:[10.1029/2006GL026894](#), 2006.

70 [van Sebille, E., Baringer, M. O., Johns, W. E., Meinen, C. S., Beal, L. M., de Jong, M. F. and van Aken, H. M.:](#) Propagation pathways of classical Labrador Sea water from its source region to 26°N, *J. of Geophys. Res., Oceans*, 116:C12027, DOI:[10.1029/2011JC007171](#), 2011.

75 [Waters, J., Lea, D. J., Martin, J., Mirouze, I., Weaver, A., and While, J.:](#) Implementing a variational data assimilation system in an operational 1/4 degree global ocean model, *Q. J. R. Meteorol. Soc.*, 141, 333–349, 2015.

Yashayaev, I. and Loder, J. W.: Further intensification of deep convection in the Labrador Sea in 2016, *Geophys. Res. Lett.*, 44, 1429–1438, DOI:[10.1002/2016GL071668](#), 2016.

Zhang, R.: Anticorrelated multidecadal variations between surface and subsurface tropical North Atlantic, *Geophys. Res. Lett.*, 34:L12713, DOI:[10.1029/2007GL030225](#), 2007.

80 Zhang, R.: Latitudinal dependence of Atlantic meridional overturning circulation variations, *Geophys. Res. Lett.*, 37:L16703, DOI:[10.1029/2010GL044474](#), 2010.

Zhang, R., Sutton, R., Danabasoglu, G., Kwon, Y.-O., Marsh, R., Yeager, S. G., Amrhein, D. E. and Little, C. M.: A review of the role of the Atlantic meridional overturning circulation in Atlantic Multidecadal Variability and associated climate impacts, *Rev. of Geophys.*, 57, 316–375, DOI:[10.1029/2019RG000644](#), 2019.

85 Zhao, J. and Johns, W. E.: Wind-driven seasonal cycle of the Atlantic meridional overturning circulation, *J. Phys. Oceanogr.*, 44, 1541–1562, DOI: [10.1175/JPO-D-13-0144.1](#), 2014a.

Zhao, J. and Johns, W. E.: Wind-forced interannual variability of the Atlantic meridional overturning circulation at 26.5°N, *J. Geophys. Res.-Oceans*, 119, 2403–2419, DOI: [10.1002/2013JC009407](#), 2014b.

90 [Zou, S. and Lozier, M. S.:](#) Breaking the linkage between Labrador Sea Water production and its export to the subtropical gyre, *Journal of Physical Oceanography*, doi: [10.1175/JPO-D-15-0210.1](#), 2016.

Formatted: Space After: 5 pt

Deleted: :[10.1126/science.1255575](#).

Moved (insertion) [10]

Moved (insertion) [11]

Formatted: Space After: 5 pt

Deleted: .

Deleted: :[10.1175/BAMS-D-16-0266.1](#).

Moved (insertion) [12]

Moved up [12]: ↕
van Sebille, E.,

Deleted: -↵

Moved up [10]: Sutton, R. T. and Dong, B.:

Deleted: Atlantic Ocean influence on a shift in European climate in the 1990s, *Nature Geosci.*, 5:788–792, DOI:[10.1038/ngeo1595](#).

Moved up [11]: 2012. →

Deleted: .

Formatted: Space After: 5 pt

Deleted: .

Deleted: .

Deleted: .

Deleted: Zou, S., Lozier, M. S. and Buckley, M.: How Is Meridional Coherence Maintained in the Lower Limb of the Atlantic Meridional Overturning Circulation?, *Geophys.*

Moved up [9]: Res. Lett.,

Deleted: 46:244-252, DOI:[10.1029/2018GL080958](#), 2019.¶

... [44]

Deleted: 17¶

Formatted: Font color: Black

Formatted ... [43]

	AMOC (Sv)	Ekman (Sv)	Florida Current (Sv)	UMO (Sv)
2004/05	18.4 ± 4.7	3.9 ± 3.7	32.0 ± 3.0	-17.5 ± 2.6
2005/06	20.9 ± 4.0	4.4 ± 2.5	32.0 ± 2.4	-15.5 ± 2.6
2006/07	20.3 ± 3.3	5.1 ± 2.9	31.6 ± 1.9	-16.3 ± 2.8
2007/08	18.9 ± 3.5	4.9 ± 2.7	31.7 ± 2.4	-17.6 ± 2.6
2008/09	18.0 ± 3.4	5.3 ± 2.8	31.6 ± 3.6	-18.7 ± 3.8
2009/10	13.5 ± 4.4	3.1 ± 3.9	30.7 ± 2.5	-20.2 ± 2.5
2010/11	17.4 ± 4.0	4.1 ± 3.4	31.1 ± 2.9	-17.6 ± 3.7
2011/12	18.0 ± 2.9	5.8 ± 2.6	31.1 ± 2.3	-18.7 ± 2.9
2012/13	14.8 ± 4.4	3.8 ± 3.5	30.8 ± 3.0	-19.6 ± 2.8
2013/14	18.0 ± 3.0	5.7 ± 2.6	31.5 ± 2.9	-19.0 ± 3.3
2014/15	17.2 ± 2.9	5.1 ± 2.6	30.4 ± 2.6	-18.2 ± 2.5
2015/16	17.5 ± 3.6	4.7 ± 2.8	31.6 ± 3.0	-18.8 ± 3.3
2016/17	18.0 ± 3.7	5.0 ± 2.7	32.4 ± 3.6	-19.4 ± 3.9
2017/18	17.8 ± 4.9	5.1 ± 3.7	30.7 ± 2.3	-17.9 ± 3.1

Table 1. The annual means of the AMOC volume transport and components in Sverdrups ($1 \text{ Sv} = 10^6 \text{ m}^3 \text{ s}^{-1}$). Values are given as the annual mean \pm the standard deviation of the 10-day binned values for that year. Annual means are computed from 1 April through 31 March. Positive values indicate northward transport, while negative values are southward. The de-correlation time is of the order of 20-30 days for all variables, and so the standard error is about square root (1/12) multiplied by the standard deviation. The de-correlation time is 20-35 days for all variables, and so the standard error is between $\sqrt{(1/18)}$ and $\sqrt{(1/10)}$ multiplied by the standard deviation.

Formatted: Font: Times New Roman

Formatted: Font: Times New Roman

Formatted Table

Deleted: MOC

Formatted: Centered

Formatted: Font: Times New Roman

Formatted: Font: Times New Roman

Formatted: Font: Times New Roman

Formatted: Font: Times New Roman

Formatted: Font: Times New Roman

Formatted: Font: Times New Roman

Formatted: Font: Times New Roman

Formatted: Font: Times New Roman

Formatted: Font: Times New Roman

Formatted: Font: Times New Roman

Formatted: Font: Times New Roman

Formatted: Font: Times New Roman

Formatted: Font: Times New Roman

Formatted: Font: Times New Roman

Formatted: Font: Times New Roman

Formatted: Font: Times New Roman

Deleted: MOC

Formatted: Font color: Auto

Deleted: 1e6

Formatted: Font color: Auto

Deleted: /

Formatted: Font color: Auto

Deleted:

Deleted:

Formatted: Font color: Auto

Formatted: Font color: Auto

Formatted: Font: 10 pt

Deleted:

Deleted:

Deleted:

Deleted:

Deleted: 18

Formatted: Font color: Black

Formatted

... [46]

... [45]

Model	AIC	AIC differences	BIC
Mean	2296.5	250.9	2304.8
Mean + CP	2193.0	147.5	2213.8
Mean + AR(1)	2082.9	37.4	2095.3
Mean + AR(1) + CP	2045.5*	0.00*	2074.6*
Trend	2255.3	209.8	2267.8
Trend + CP	2175.8	130.3	2204.9
Trend + AR(1)	2068.3	22.8	2085.0
Trend + AR(1) + CP	2068.3	22.8	2085.0

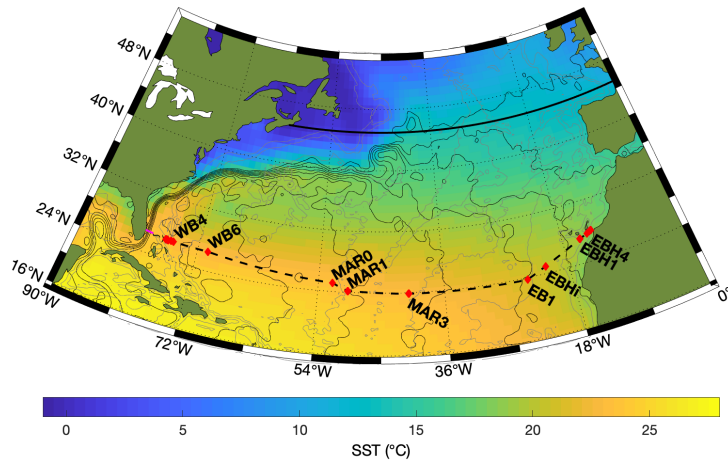
85 **Table 2.** Comparison of the eight models fitted to the AMOC-Ekman time series. The Akaike Information Criterion (AIC) and Bayesian Information Criterion (BIC) obtained for each model are presented. The most appropriate model from these information criterion is selected as the smallest and highlighted with a *. The AIC differences between each model fitted and the “best model” (with the smallest AIC) are also presented. The differences are all large (>10), indicating that there is no other model amongst those compared that fits the data reasonably well. Note that because no changepoints were detected under the

90 Trend + AR(1) + CP model, the AIC and BIC are the same as the Trend + AR(1) model.

Deleted: 19*

Formatted: Font color: Black

Formatted: Normal, Border: Top: (No border), Bottom: (No border), Left: (No border), Right: (No border), Between : (No border), Tab stops: 7.96 cm, Centered + 15.92 cm, Right

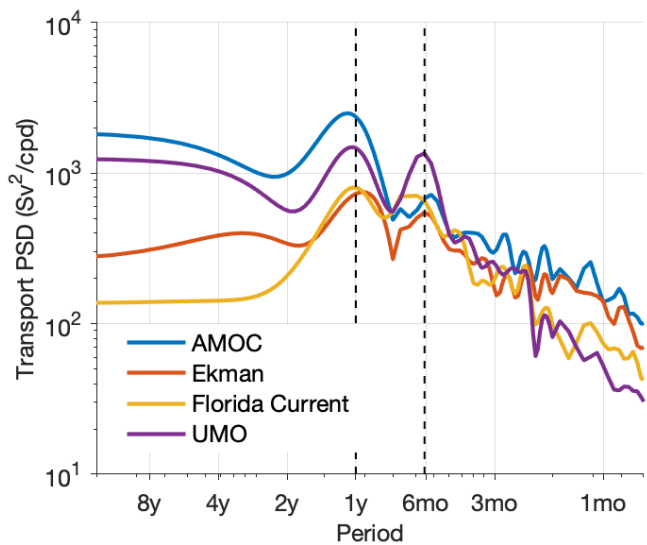


95 **Figure 1** The RAPID 26°N array traverses the subtropical gyre of the North Atlantic. The magenta line shows the location of
the subsea cable in the Florida Strait and red diamonds connected by a dashed black line show the location of moorings. ‘WB’,
‘MAR’, and ‘EB’ denote, respectively, moorings in the western boundary, mid-Atlantic Ridge and eastern boundary sub-
arrays. For clarity, not all moorings are labelled. The colour shows mean sea surface temperature (SST) in March (average of
100 1999 to 2018) and the continuous black lines are the corresponding contours of sea surface height (contour interval 0.1m).
Contours of water depth at 1000, 3000 and 5000 m are shown in grey. The thick black line at 45°N indicates where multiple
data sources have been used to estimate the AMOC at the boundary between the subtropical and subpolar gyres (Desbruyères
et al., 2019).

Deleted: 20

Formatted: Font color: Black

Formatted: Normal, Border: Top: (No border), Bottom: (No border), Left: (No border), Right: (No border), Between : (No border), Tab stops: 7.96 cm, Centered + 15.92 cm, Right



05 **Figure 2** Power spectral density of the AMOC and its component parts as a function of period. The vertical dashed lines highlight the annual and semiannual frequencies.

This zoomed-in view shows the PSD for periods of 8 years and 4 years. The AMO (blue) and UMO (purple) series show a slight decrease in PSD as the period increases from 8y to 4y. The Ekma (orange) series shows a slight increase. The Floric (yellow) series remains relatively constant.

Deleted: 21

Formatted: Font color: Black

Formatted: Normal, Border: Top: (No border), Bottom: (No border), Left: (No border), Right: (No border), Between : (No border), Tab stops: 7.96 cm, Centered + 15.92 cm, Right

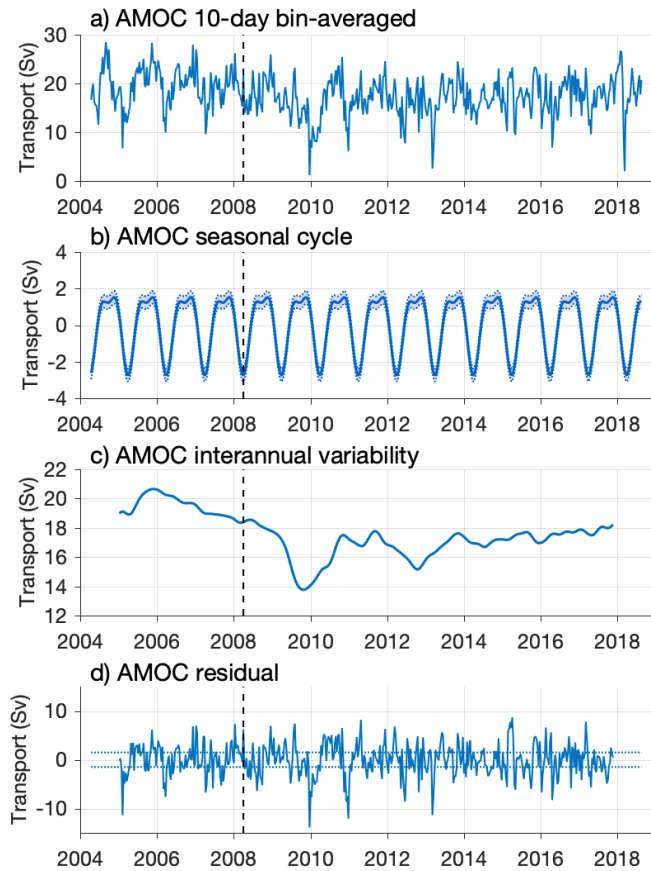
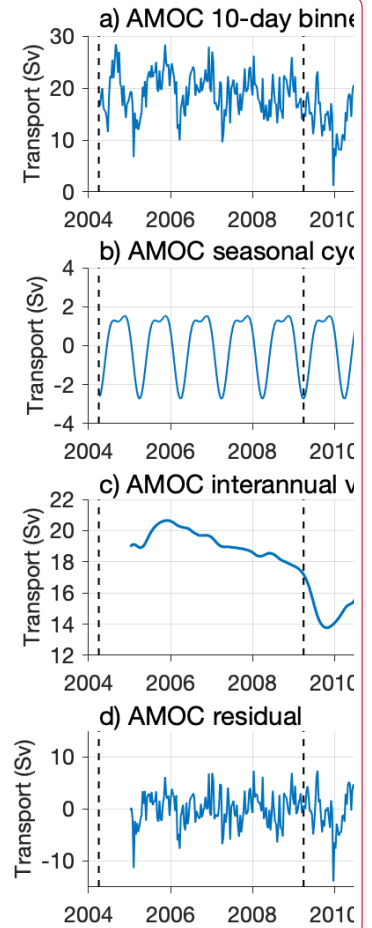


Figure 3 The total AMOC at 10-day resolution (a), can be decomposed into a seasonal cycle (b), interannual variability (c), and a residual (d). The interannual component is obtained by filtering the data with a 540-day low-pass filter after removal of the mean seasonal cycle. In (b) the dotted lines show the annual cycle \pm one standard error, and the dotted lines in (d) are ± 1.5 Sv the estimated error of 10-day binned data.



Deleted:

Formatted: Font color: Auto

Formatted: Line spacing: Double

Deleted: 22

Formatted: Font color: Black

Formatted: Normal, Border: Top: (No border), Bottom: (No border), Left: (No border), Right: (No border), Between: (No border), Tab stops: 7.96 cm, Centered + 15.92 cm, Right

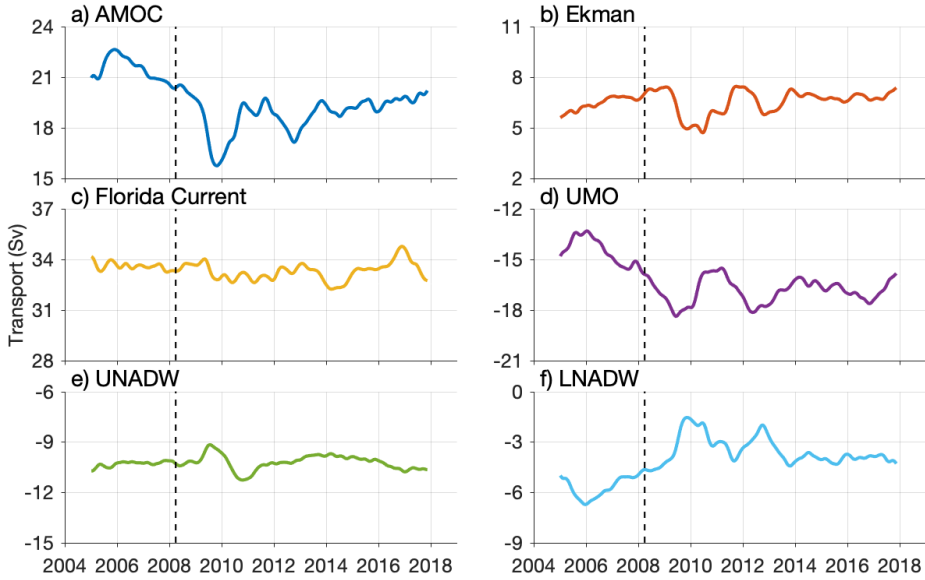
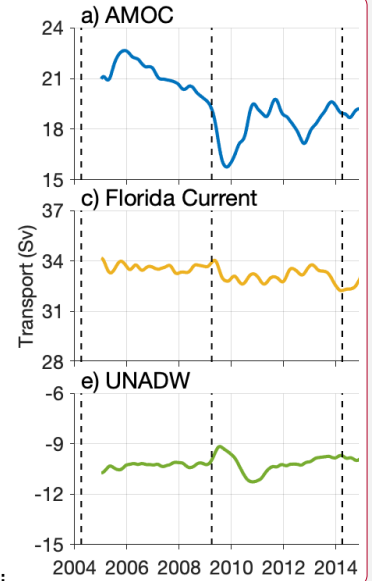
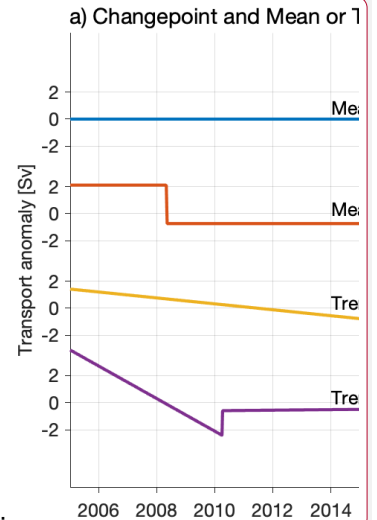


Figure 4 Interannual variability of the AMOC at 26°N and its component parts: (a) AMOC, (b) Ekman, (c) Florida Current, (d) Upper mid-ocean (UMO), (e) Upper North Atlantic Deep Water (UNADW), and (f) Lower North Atlantic Deep Water (LNADW).



Deleted:

Deleted: ..., (UMO), (e) Upper North Atlantic Deep Water, (UNADW), and (f) Lower North Atlantic Deep Water... [47]

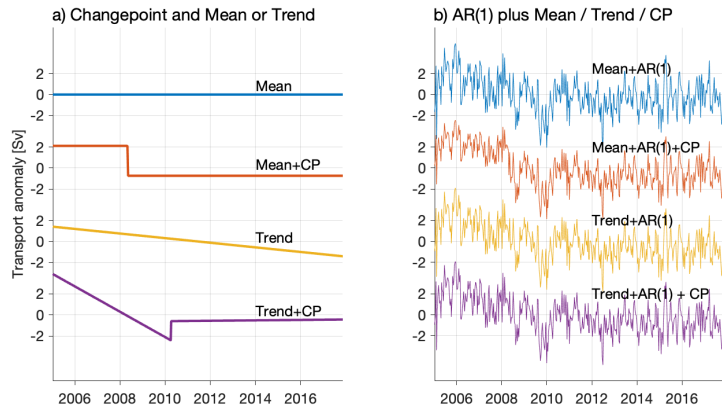


Deleted:

Deleted: 23

Formatted: Font color: Black

Formatted: Normal, Border: Top: (No border), Bottom: (No border), Left: (No border), Right: (No border), Between : (No border), Tab stops: 7.96 cm, Centered + 15.92 cm, Right



40 **Figure 5** Changepoint analysis of the AMOC-Ekman time series. In panel (a), only a mean or a trend, with or without a changepoint are fit. In panel (b), an AR(1) is also fit. The model with the best overall fit is the Mean + AR(1) + CP model (red, right) according to the AIC (see Table 2), indicating that the time series can best be explained by an AR(1) time series with a change in the mean in 2008.

Deleted: 2009.

Deleted: 24

Formatted: Font color: Black

Formatted: Normal, Border: Top: (No border), Bottom: (No border), Left: (No border), Right: (No border), Between : (No border), Tab stops: 7.96 cm, Centered + 15.92 cm, Right

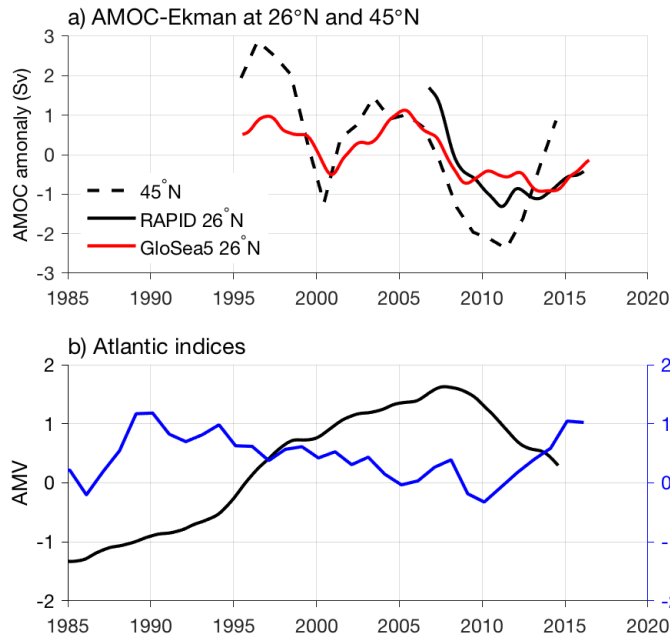
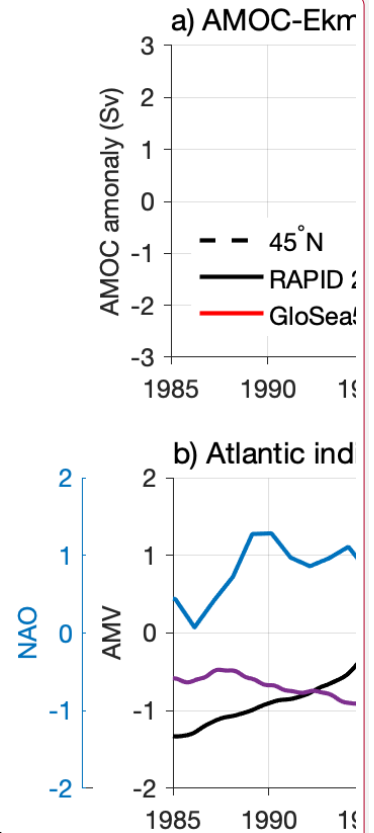


Figure 6 (a) AMOC anomalies from RAPID at 26°N (black, Sv), 26°N GloSea5 reanalysis (red, Sv), AMOC 45°N (black dashed, Sv). b) The AMV (black) and NAO (blue). The AMV has been decadal low-pass filtered, with a 5-year low-pass filter applied to the NAO time series. The Ekman transport has been removed from the AMOC time series.



Deleted:

Deleted: ,

Deleted:) and subpolar North Atlantic (80°W to 20°E, 45°N to 67°N) full depth ocean heat content anomaly (purple, 10²² J).

Deleted: other

Formatted: Font color: Black

Formatted: Normal, Space After: 10 pt, Border: Top: (No border), Bottom: (No border), Left: (No border), Right: (No border), Between : (No border)

Deleted: 25

Formatted: Font color: Black

Formatted: Normal, Border: Top: (No border), Bottom: (No border), Left: (No border), Right: (No border), Between : (No border), Tab stops: 7.96 cm, Centered + 15.92 cm, Right

Page 1: [1] Formatted Moat, Ben 5/18/20 1:01:00 PM

Font color: Black

Page 1: [2] Formatted Moat, Ben 5/18/20 1:01:00 PM

Normal, Border: Top: (No border), Bottom: (No border), Left: (No border), Right: (No border), Between : (No border),
Tab stops: 7.96 cm, Centered + 15.92 cm, Right

Page 8: [3] Formatted Moat, Ben 5/18/20 1:01:00 PM

Font: Times New Roman

Page 8: [4] Formatted Moat, Ben 5/18/20 1:01:00 PM

Space After: 5 pt

Page 8: [5] Formatted Moat, Ben 5/18/20 1:01:00 PM

Font: Times New Roman

Page 8: [5] Formatted Moat, Ben 5/18/20 1:01:00 PM

Font: Times New Roman

Page 8: [6] Deleted Moat, Ben 5/18/20 1:01:00 PM

▼

Page 8: [7] Formatted Moat, Ben 5/18/20 1:01:00 PM

Font: Times New Roman

Page 8: [8] Formatted Moat, Ben 5/18/20 1:01:00 PM

Font: Times New Roman

Page 8: [9] Formatted Moat, Ben 5/18/20 1:01:00 PM

Font: Times New Roman

Page 8: [10] Formatted Moat, Ben 5/18/20 1:01:00 PM

Font: Times New Roman

Page 8: [11] Formatted Moat, Ben 5/18/20 1:01:00 PM

Font: Times New Roman

Page 8: [12] Deleted Moat, Ben 5/18/20 1:01:00 PM

▼

Page 8: [13] Formatted Moat, Ben 5/18/20 1:01:00 PM

Font: Times New Roman

Page 8: [13] Formatted Moat, Ben 5/18/20 1:01:00 PM

Font: Times New Roman

▼

Page 8: [15] Formatted	Moat, Ben	5/18/20 1:01:00 PM
-------------------------------	------------------	---------------------------

Font: Times New Roman

Page 8: [16] Deleted	Moat, Ben	5/18/20 1:01:00 PM
-----------------------------	------------------	---------------------------

▼

Page 8: [17] Formatted	Moat, Ben	5/18/20 1:01:00 PM
-------------------------------	------------------	---------------------------

Font: Times New Roman

Page 8: [17] Formatted	Moat, Ben	5/18/20 1:01:00 PM
-------------------------------	------------------	---------------------------

Font: Times New Roman

Page 8: [18] Formatted	Moat, Ben	5/18/20 1:01:00 PM
-------------------------------	------------------	---------------------------

Font: Times New Roman

Page 8: [19] Formatted	Moat, Ben	5/18/20 1:01:00 PM
-------------------------------	------------------	---------------------------

Font: Times New Roman

Page 8: [20] Formatted	Moat, Ben	5/18/20 1:01:00 PM
-------------------------------	------------------	---------------------------

Font: Times New Roman

Page 8: [21] Deleted	Moat, Ben	5/18/20 1:01:00 PM
-----------------------------	------------------	---------------------------

▼

Page 8: [22] Formatted	Moat, Ben	5/18/20 1:01:00 PM
-------------------------------	------------------	---------------------------

Font: Times New Roman

Page 8: [23] Formatted	Moat, Ben	5/18/20 1:01:00 PM
-------------------------------	------------------	---------------------------

Font: Times New Roman

Page 8: [24] Formatted	Moat, Ben	5/18/20 1:01:00 PM
-------------------------------	------------------	---------------------------

Font: Times New Roman

Page 8: [24] Formatted	Moat, Ben	5/18/20 1:01:00 PM
-------------------------------	------------------	---------------------------

Font: Times New Roman

Page 8: [25] Formatted	Moat, Ben	5/18/20 1:01:00 PM
-------------------------------	------------------	---------------------------

Font: Times New Roman

Page 8: [26] Formatted	Moat, Ben	5/18/20 1:01:00 PM
-------------------------------	------------------	---------------------------

Font: Times New Roman

Page 8: [26] Formatted	Moat, Ben	5/18/20 1:01:00 PM
-------------------------------	------------------	---------------------------

Page 8: [27] Formatted Moat, Ben 5/18/20 1:01:00 PM

Font: Times New Roman

Page 8: [28] Formatted Moat, Ben 5/18/20 1:01:00 PM

Font: Times New Roman

Page 8: [28] Formatted Moat, Ben 5/18/20 1:01:00 PM

Font: Times New Roman

Page 8: [29] Deleted Moat, Ben 5/18/20 1:01:00 PM

▼

Page 8: [30] Formatted Moat, Ben 5/18/20 1:01:00 PM

Font: Times New Roman

Page 8: [31] Deleted Moat, Ben 5/18/20 1:01:00 PM

▼

Page 8: [32] Formatted Moat, Ben 5/18/20 1:01:00 PM

Font: Times New Roman

Page 8: [33] Formatted Moat, Ben 5/18/20 1:01:00 PM

Font: Times New Roman

Page 8: [34] Formatted Moat, Ben 5/18/20 1:01:00 PM

Font: Times New Roman

Page 8: [35] Formatted Moat, Ben 5/18/20 1:01:00 PM

Font: Times New Roman

Page 1: [36] Formatted Moat, Ben 5/18/20 1:01:00 PM

Normal, Border: Top: (No border), Bottom: (No border), Left: (No border), Right: (No border), Between : (No border),
Tab stops: 7.96 cm, Centered + 15.92 cm, Right

Page 10: [37] Deleted Moat, Ben 5/18/20 1:01:00 PM

▼

Page 10: [38] Deleted Moat, Ben 5/18/20 1:01:00 PM

▼

Page 10: [39] Deleted Moat, Ben 5/18/20 1:01:00 PM

▼

Page 10: [40] Deleted Moat, Ben 5/18/20 1:01:00 PM

▼

Normal, Border: Top: (No border), Bottom: (No border), Left: (No border), Right: (No border), Between : (No border),
Tab stops: 7.96 cm, Centered + 15.92 cm, Right

Page 11: [42] Deleted **Moat, Ben** **5/18/20 1:01:00 PM**



Page 1: [43] Formatted **Moat, Ben** **5/18/20 1:01:00 PM**

Normal, Border: Top: (No border), Bottom: (No border), Left: (No border), Right: (No border), Between : (No border),
Tab stops: 7.96 cm, Centered + 15.92 cm, Right

Page 17: [44] Deleted **Moat, Ben** **5/18/20 1:01:00 PM**



Page 1: [45] Formatted **Moat, Ben** **5/18/20 1:01:00 PM**

Normal, Border: Top: (No border), Bottom: (No border), Left: (No border), Right: (No border), Between : (No border),
Tab stops: 7.96 cm, Centered + 15.92 cm, Right

Page 18: [46] Deleted **Moat, Ben** **5/18/20 1:01:00 PM**



Page 23: [47] Deleted **Moat, Ben** **5/18/20 1:01:00 PM**



Page 23: [47] Deleted **Moat, Ben** **5/18/20 1:01:00 PM**



Page 23: [47] Deleted **Moat, Ben** **5/18/20 1:01:00 PM**

